Methods for Analyzing Power System Small Signal Stability

By

Dan Lin, B. Eng.

A thesis submitted to the school of Graduate Studies

in partial fulfillment of the requirements for the

degree of Master of Engineering

Faculty of Engineering and Applied Science

Memorial University of Newfoundland

May 2015

St. John's Newfoundland and Labrador Canada

Abstract

Small disturbance such as load changes will affect stability of power systems. Small signal stability problem refers to the stability problems caused by small disturbances. Power oscillation appears in the system because of the effect of small disturbances. Oscillation's property is the key to analyze the stability of power system. The undamped power oscillation may cause the blackout, such as the power outage of North American Western Interconnected (WSCC) System happened in 1996.

In order to learn the oscillation's mode, two methods are applied to analyze the oscillation caused by small disturbances. The first method is referred to as model-based analysis for small signal stability problem. It uses mathematical model to indicate whether the system is stable based on the eigenvalue calculation for the mathematical model. The other method is the measurement-based analysis for power system. This method is more popular for today's power system analysis. It uses real-time synchrophasor measurement collected from Phasor Measurement Units (PMUs) that are installed at various buses to estimate the mode of oscillations based on prony method. This method requires the system to be visible using PMUs. In addition, the mode of oscillation for every bus can be detected with the time stamp.

This thesis studies these two methods to analyze different power systems. The advantages of using measurement-based analysis are clearly shown in this research.

As the power system is highly dynamic, model-based analysis cannot provide accurate real-time information. However, the challenge for applying measurement-based analysis is to find the optimum locations for installing PMUs so that non-observable area does not exist in the whole system. Case studies using four different power system models are presented throughout the thesis.

Acknowledgements

I am heartily grateful to my supervisor, Dr. Benjamin Jeyasurya. His encouragement and support for my research makes me confident and motivated to continue the work. I would like to appreciate the financial support from Natural Sciences and Engineering Research Council of Canada and Memorial University of Newfoundland. I could not finish this research without them. Finally, I am thankful to all the friends that have helped me with my thesis.

Table of Contents

Abstract ..... **i**

Acknowledgements ..... **iii**

Contents ..... **iv**

List of Figures ..... **vii**

List of Tables ..... **x**

List of Abbreviations and Symbols ..... **x**

1. Introduction 1

    1.1 Background of the Research 1

    1.2 Objectives of the Research 2

    1.3 Organization of the Thesis 3

2. Power System Small Signal Stability 5

    2.1 Introduction 5

    2.2 Overview of Power System Stability 5

    2.3 Small Signal Stability Problem in Power System 6

    2.4 Case Study of Two-Area Power System Small Signal Stability 12

    2.5 Conclusion 14

3. Model-Based Analysis for Power System Small Signal Stability 15

    3.1 Introduction 15

3.2 Model-based Analysis 16
3.2.1 Eigenvalue Analysis 16
3.2.2 Model-Based Analysis of Systems with Automatic Voltage Regulator 18
3.2.3 Case Study of Model Analysis for The Systems With AVR 23
3.2.4 Small Signal Stability Analysis Of Systems With Power System Stabilizer 28
3.2.5 Case Study of Model Analysis for the System with PSS 32
3.3 Conclusion 36
4. Wide - Area Measurement System (WAMS) 38
4.1 Introduction 38
4.2 Phasor Measurement Unit 39
4.2.1 Principle of Phasor Measurement Unit 40
4.2.2 Application of PMUs 43
4.2.3 Estimation in PMUs 46
4.3 Case Study of Signal Estimation 49
4.4 Case Study of Applying DFT to Obtain Phasor 53
4.5 Conclusion 54
5. Measurement-Based Analysis for Power System Small Signal Stability 56
5.1 Introduction 56
5.2 Measurement-Based Analysis 58
5.2.1 Principle of Prony Method 58

5.2.2 Case Study of Measurement-Based Analysis for Two-Area System 61

5.3 Test Systems and Tools for Study 64

5.3.1 68-Bus Power System 64

5.3.2 39-Bus Power System 65

5.2.3 Tools for Study 66

5.3 Case Studies 67

5.3.1 Measurement-based analysis for 68-bus power system 67

5.3.2 Measurement-Based Analysis for 39-Bus Power System 74

5.4 Measurement-Based Analysis Technique's Deployment in Power System 78

5.5 Conclusion 80

6. Conclusion and Future Works 81

6.1 Conclusions 81

6.2 Contribution of the Thesis 82

6.3 Future Works 82

References 84

Appendix A: Data for Two-Area Power System 88

Appendix B: Data for the 4 × 555 MVA Power System 90

Appendix C: Data for The IEEE 14-Bus Power System 91

Appendix D: Data for the 68-Bus Power System 94

Appendix E: Data for the 39-Bus Power System 97

Conference Papers duing the MEng Program 102

List of Figures

Figure 2.1 Classification of Power System Stability 7

Figure 2.2 Model of Small Signal Stability Analysis 10

Figure 2.3 Single Line Diagram of Two-Area Power System 13

Figure 2.4 Speed of Generator #1 and #2 After the Disturbance 13

Figure 3.1 General Working Process of Excitation System 20

Figure 3.2 Block Diagram of The System With Excitation System 22

Figure 3.3 Single Line Diagram 24

Figure 3.4 Thyristor Excitation System 24

Figure 3.5 Block Diagram of PSS 30

Figure 3.6 Block Diagram of The System With PSS 31

Figure 3.7 Single Line Diagram of IEEE 14-Bus System 33

Figure 3.8 Speed of Generators With Disturbance In IEEE 14-Bus System With AVR 34

Figure 3.9 Eigenvalues for the 14-Bus system with AVR 34

Figure 3.10 Rotor Speed Variation of Generators With Disturbance In IEEE 14-Bus System With PSS 35

Figure 3.11 Eigenvalues for the 14-Bus System with PSS 36

Figure 4.1 Basic Architecture of Phasor Measurement Unit 41

Figure 4.2 Application of PMUs in WAMS 45

Figure 4.3 Expression of Pure Sinusoidal Signal In The Time Scale 47

Figure 4.4 Phasor Expression of Pure Sinusoidal Signal 47

Figure 4.5 Sample Windows For Phasor Estimation In DFT 49

Figure 4.6 Expression of the Signal in Both Frequency Domain and Time Domain..... 51

Figure 4.7 Comparison of The Original Signal and The Estimated Signal ... 52

Figure 5.1 Voltage Magnitude of Bus #7 and #9 in Two-Area System 61

Figure 5.2 Prony Estimation for Voltage Magnitude at Bus #7 62

Figure 5.3 Damping Coefficient Detected by Prony Method 63

Figure 5.4 Single Line Diagram of 68-Bus Power System 64

Figure 5.5 Single Line Diagram for 39-Bus Power System 66

Figure 5.6 Phasor Variation of Voltages for Bus 1, 2, 18, 47, 48 69

Figure 5.7 Phasor of Voltage for Bus 2 69

Figure 5.8 Voltage Magnitude of Bus 2 70

Figure 5.9 Line current Magnitude of Bus 2 70

Figure 5.10 Apparent Power through Bus 2 and Bus 1 71

Figure 5.11 Real Power through Bus 2 and Bus 1 72

Figure 5.12 Reactive Power through Bus 2 and Bus 1 72

Figure 5.13 Damping for Phasors of Bus Voltages in 68-Bus Power System . 74

Figure 5.14 Voltage Magnitude at Bus 3..... 75

Figure 5.15 Bus Magnitude at Bus 4..... 76

Figure 5.16 Frequency for the Oscillations at Bus 3, 4..... 77

Figure 5.17 Damping for Bus Voltages at Bus 3, 4..... 77

Figure 5.18 Simplified Flowchart for OMS 80

Figure A.1 Single Line Diagram of the Two-Area Power System 88

Figure B.1 Single Line Diagram of 4×555 MVA System 90

Figure C.1 Single Line Diagram of IEEE 14-Bus Power System 92

Figure E.1 Single Line Diagram of 39-Bus Power System 97

List of Tables

Table 3.1 Variation of Damping and Synchronized Coefficient 27

Table 4.1 Application of PMUs in Power System 44

Table 4.2 Discrete Fourier Transform of 100 Samples in One Window 50

Table 4.3 Phasor of Voltage Signal With Non-recursive Phasor Estimation 54

Table 5.1 PMUs' Placement for 68-bus Power System 65

Table 5.2 PMUs' Placement for 39-bus Power System 66

Table A.1 Power Flow Results for Two-Area System 89

Table B.1 Constants for the 4×555 MVA System 90

Table C.1 Constant PQ Load Information for IEEE 14-Bus System 93

Table D.1 Load Information for the 68-Bus Power System 94

Table D.2 Synchronous Machine Information for 68-Bus Power System 96

Table E.1 Bus Data for 39-Bus Power System 98

Table E.2 Load Data for 39-Bus Power System 100

Table E.3 Generator Data for 39-Bus Power System 101

List of Abbreviations and Symbols

DFT : Discrete Fourier Transform

Hz : Herz

PMU : Phasor Measurement Unit

AVR : Automatic Voltage Regulator

PSS : Power System Stabilizer

DC : Direct Current

AC : Alternating Current

OEL : Over Excitation Limiter

UEL : Under Excitation Limiter

SCADA : Supervisory Control and Data Acquisition

WAMS : Wide - Area Measurements System

DAE : Linearized Differential Algebraic Equation

GPS : Global Position System

PDC : Phasor Data Concentrator

MW : Mega Watt

MVar : Mega Volta Ampere Reactive

MVA : Mega Volt Ampere

VAR : Volt-Ampere Reactive

Chapter 1

Introduction

1.1 Background of the Research

Small signal disturbances has been in power system of great concern for years. It can lead the power oscillation in power system, which could result in blackout. The accident happened in 1996, WSCC system (North American Western Interconnected System) occurred the inter-area oscillation with the frequency at 0.23 Hz. The whole system broke up [41].

Conventional method of analyzing power system's small signal stability like model-based analysis has been applied for years. However, it could not detect the real-time behavior of power system. The mathematical model of power system for model-based analysis cannot remain the same all the time. It requires large computing space. The operators will not find the problems if there is increasing oscillations. The early prediction of power system's behavior is necessary for protecting the system. In addition, model-based analysis cannot collect the information from other systems. However, the power systems are interconnected; the mode for the interconnected system is needed [5].

In order to meet the current requirement for power system monitoring, measurement-based analysis is introduced to solve these problems. The method is applied to power system based on installing phasor measurement units to the system, which can directly detect the real-time value and predict the trend of the oscillation in power system. This new technique is widely applied to power system to monitor the oscillation status and has been broadly studied [15].

This thesis provides the comparison of two methods: model-based analysis and measurement-based analysis. The methods will provide their own approach to obtain the analysis for the oscillations happened in power system. The approaches used in the two method are eigenvalue analysis for model-based analysis, Discrete Fourier Transform (DFT) method and prony method for measurement-based analysis [5].

1.2 Objectives of the Research

Obtain the real-time mode of oscillation and predict the future values when small signal disturbances happen can avoid the potential accident in power system. Traditional method of using eigenvalue analysis can only determine whether a system is stable or not for one specific time. By applying DFT method, it simulates the original signal with phasor. The phasor is one of the important elements to study the stability. The phasor is collected with the time-stamp from different locations, and it is called synchrophasor. Synchrophasor is then used as the sample data for prony analysis to detect the mode of oscillations. Prony analysis will give the damping and frequency for oscillations based on these data. The system's behavior is analyzed

throughout the whole procedures. The main objectives of this research are listed as below:

1. Study the techniques that are used in analyzing power system's small signal stability problem

2. Compare the two methods for detecting the mode power oscillation and the stability for power system. The two methods are model-based analysis and measurement-based analysis.

3. Represent the mathematical model that is used for model-based analysis, this mathematical model is derived through a classic system model, and the procedure of calculating the eigenvalue of the system is also provided.

4. Describe the principles used in the two methods and use various case studies to determine the performances of the two methods. The indices of good performance includes the time that is used for indicating the stability and the continuity of analyzing.

5. Discuss the advantages of measurement-based analysis by giving the theory of PMUs. Since measurement-based analysis is based on installing PMUs to the system. Synchrophasor technology that is used in PMUs is the backbone of the analysis. Study the principles of PMUs will give the deep understanding for the reasons of applying this technique to power system.

1.3 Organization of the Thesis

Chapter 2 illustrates power system small signal stability, the factors that cause

small signal stability problem and the reasons to study it. Two-area power system is used to describe the phenomenon of small disturbance and the system's performance.

Chapter 3 describes model-based analysis. The mathematical model used in model-based analysis is discussed in this chapter, including the system with only Automatic Voltage Regulator (AVR) and the system with both AVR and Power System Stabilizer (PSS). The 14-Bus power system is used to learn the model-based method's performance for the two situations described above.

Chapter 4 focuses on the theory of PMUs and its function. PMUs are the foundamental element to apply measurement-based analysis. One numerical case study is applied to support the understanding of DFT method. Another case study of applying non-recursive method to get phasor from bus voltage is described. This chapter also gives the further application for PMUs.

Chapter 5 gives the theory of applying measurement-based analysis. Two-area power system illustrates the application of measurement-based analysis. This chapter describes how measurement-based analysis is applied to wide-area system. This chapter applies the method to a 68-bus power system and 39-bus power system, the analysis initiated from calculating phasor, to the computing of power flow using the phasor collected from PMUs, finally obtain the damping and frequency through prony method.

Chapter 6 provides the suggestions for the future research work and concludes the main points for this thesis.

Chapter 2

Power System Small Signal Stability

2.1 Introduction

This chapter introduces the power system small signal stability. Section 2.2 gives the overview of power system stability. Section 2.3 presents the small signal problem in power system, including the results that this problem can lead. The definition of small signal stability and the causes for the instability are described. Section 2.4 provides a case study for presenting the nature of small signal stability problem. The simulations are given for both before the disturbance and after the disturbance in this section. Section 2.5 concludes this chapter.

2.2 Overview of Power System Stability

Power system stability performance also depends on if the system operates normally when disturbances happen. The disturbance can be either large or small, small disturbances refers to the load changes, large disturbances could be short circuit short on transmission lines or the loss of the tie between two subsystems. Power system stability problems are classified as rotor angle stability, frequency stability, and

voltage stability. Rotor angle stability includes two major categories: small signal stability and transient stability. This thesis mainly discuss small signal stability problem [3].

2.3 Small Signal Stability Problem in Power System

Small signal stability problems exist in power system for many decades. The system oscillates with undamped or growing phenomenon because of lacking of damping or synchronism. The unstable oscillations could appear as one generator or a small part against the rest of the power system or the whole interconnected power system. The problem in this situation is called local mode problem. On the other hand, the inter-area mode problem which refers to the interconnected power system's unstable oscillation, is well represented by the WSCC system (North American Western Interconnected System) incident happened in 1996, the circuits outages causes the low frequency oscillation as inter-area mode. It results in the outage of the whole power system [1].

Small signal stability refers to the ability to maintain synchronism when small disturbances happen. The disturbances are considered very small, so the equations to present the system state need to be linearized when study. Small disturbance angle stability and transient stability are both related to rotor angle changes. Small signal stability and transient stability belong to the rotor angle stability which follows the classification of the stability problem for power system shown in Figure 2.1 [2]. Power system stability problem has three categories: rotor angle stability, frequency

stability and voltage stability.

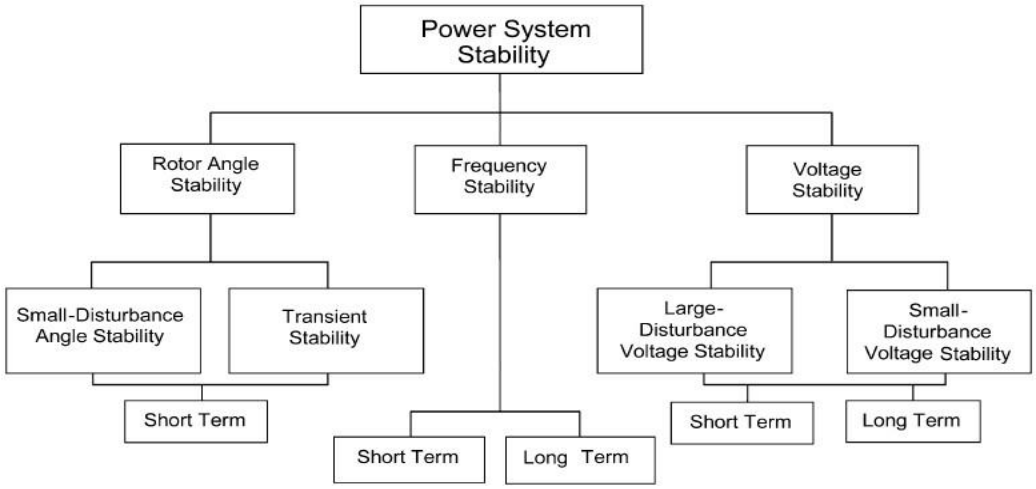

Figure 2.1 Classification of Power System Stability [2]

Electromechanical oscillation in power system is studied in the area of rotor angle stability problem, the oscillation exists because of the behavior that the synchronous generators' power outputs are related to the variation of rotor angles. As the generators' electromagnetic torque is constant and equal to the mechanical power, the sudden change of electromagnetic torque caused by the disturbance such as a fault on the line will result in the additional energy to promote or weaken the rotor's motion of generators. When considering the interconnected generators, some of the synchronous generators can lose synchronism if a disturbance occurs. The slower synchronous generator will transfer the partial power to the other generators. The disturbance can result in two kinds of unstable oscillation, one is the insufficient synchronism which relates to the rotor angle deviation, the other one is insufficient damping which relates to the rotor speed deviation. Lack of damping is the main problem that exists in small signal stability and results in undamped oscillation in power system [2].

Under the small disturbance, the small signal stability problem can be either local or global. Local mode commonly refers to the rotor oscillation that happens in one generator against the rest of generators. On the contrary, the global mode happens among the large group of generators that are connected to each other. The frequency for local mode usually is in the range of 1-3 Hz. For the global mode, the frequency usually is usually in the range of 0.3-0.8 Hz [3, 4].

Power system is a dynamic and nonlinear system. State of the system is the instant information that is necessary for the system to get the next performance. It combines the different inputs of the information of a system. The states change from time to time. It can be chosen from any physical variables. State-space is a method to understand power system from n dimensions.

Power system can be expressed by m th order nonlinear differential equations given by:

$$\dot{x}_i = f_i(x_1, x_2, ..., x_m; u_1, u_2, ..., u_q; t) \tag{2.1}$$

Where x refers to the states of the system at different time, u is the input of the system, t is noted as time, $\dot{x}$ is the state differential variables along with the time. In addition, the state and the input are usually written as the vector format like follows:

$$x = \begin{bmatrix} x_1 \\ x_2 \\ ... \\ x_m \end{bmatrix} \tag{2.2}$$

$$u = \begin{bmatrix} u_1 \\ u_2 \\ \dots \\ u_q \end{bmatrix} \tag{2.3}$$

$$f = \begin{bmatrix} f_1 \\ f_2 \\ \dots \\ f_m \end{bmatrix} \tag{2.4}$$

The system's output is used to determine whether the system is stable or not. Output should contain the state and the input of the system. Based on the understanding of the output, the expression of it is given below:

$$y = g(x,u) \tag{2.5}$$

From Equation (2.5), y and g are also written as the vectors as:

$$y = \begin{bmatrix} y_1 \\ y_2 \\ \dots \\ y_l \end{bmatrix} \tag{2.6}$$

$$g = \begin{bmatrix} g_1 \\ g_2 \\ \dots \\ g_l \end{bmatrix} \tag{2.7}$$

Where g is the vector to indicate the relation between the output and the input.

$\dot{x}$ from Equation (2.1) represents the change of a state. Therefore, when discuss the steady state of a system, it means there is no change of the state. $\dot{x}$ at any time is zero when a system becomes steady. The state at the time when $\dot{x}$ equals to zero is determined as equilibrium point. For power system, the equilibrium point will be more than one because of the nonlinear property.

The model to analyze power system's stability refers to a single machine connected to the infinite bus system. In addition, all the resistances are neglected to simplify the analysis. Figure 2.2 shows the model [4].

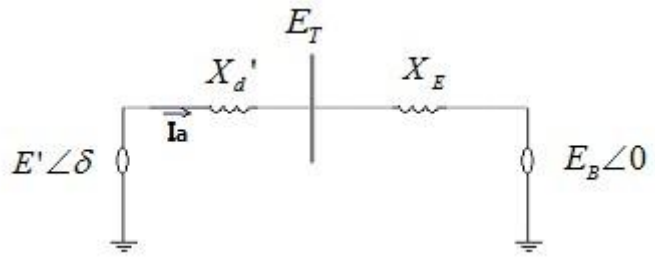

Figure 2.2 Model of Small Signal Stability Analysis [4]

Since all the resistances are neglected, $E'\angle\delta$ represents the voltage before the transient reactance X_d'. The system at receiving end is connected through the reactance of X_E and the voltage at the receiving end is $E_B\angle 0$. E_T is the terminal voltage of the stator, I_a is the current of this system. E' leads E_B δ degree. The relationships are presented as follows:

$$I_a = \frac{E'\angle 0 - E_B\angle\delta}{j(X_d' + X_E)} \tag{2.8}$$

Assume $X_d' + X_E = X_T$ in Equation (2.8), then the power generated from sending end is expressed as below, I_a^* is the conjugate form of I_a.

$$S_S = E' \bullet I_a^* = \frac{E' E_B \sin\delta}{X_T} + j\frac{E'(E' - E_B \cos\delta)}{X_T} \tag{2.9}$$

Since all the resistance are neglected, then we have:

$$T_e = \frac{E' E_B}{X_T} \sin\delta \tag{2.10}$$

T_e is the air gap torque of the generator from Equation (2.10). In order to perform small change of the system. The change of air gap torque is noted as ΔT_e, the initial state of rotor angle is δ_0. The relation is represented as follow:

$$\Delta T_e = \frac{\partial T_e}{\partial \delta}\Delta\delta = \frac{E'E_B}{X_T}\cos\delta_0(\Delta\delta) \tag{2.11}$$

Where $\Delta\delta$ is the change of rotor angle. In order to linearize the system around the initial point, the motion equation is used here to analyze.

$$\frac{d\Delta\omega_r}{dt} = \frac{1}{2H}(T_m - T_e - K_D\Delta\omega_r) \tag{2.12}$$

Motion equation is shown in Equation (2.12), where H is inertia constant, K_D is the damping coefficient which is important when detect the system, ω_r refers to angular velocity of the rotor in electrical rad/s and ω_0 is the rated value of ω_r. Substitute Equation (2.11) when linearize Equation (2.12), the expression should be like follows:

$$\frac{d\Delta\omega_r}{dt} = \frac{1}{2H}[\Delta T_m - K_s\Delta\delta - K_D\Delta\omega_r] \tag{2.13}$$

In Equation (2.13), $K_s = \frac{E'E_B}{X_T}\cos\delta_0$ because of previous derivation. The angle's position has the relation as below:

$$\frac{d\delta}{dt} = \omega_0\Delta\omega_r \tag{2.14}$$

Express the Equation (2.13) and (2.14) in matrix form,

$$\begin{bmatrix} \Delta\dot{\omega} \\ \Delta\dot{\delta} \end{bmatrix} = \begin{bmatrix} -\frac{K_D}{2H} & -\frac{K_S}{2H} \\ \omega_0 & 0 \end{bmatrix}\begin{bmatrix} \Delta\omega_r \\ \Delta\delta \end{bmatrix} + \begin{bmatrix} \frac{1}{2H} \\ 0 \end{bmatrix}\Delta T_m \tag{2.15}$$

Equation (2.15) is also expressed as the form of $\dot{x} = Ax + bu$. Where x is the state of

system and u is the input of system. According to the matrix, damping relates to the speed deviation, synchronism corresponds with rotor angle deviation. When analyzing small signal stability problems, the damping ratio and synchronism are the indices to evaluate the behavior of power system. This model will support the study of how to use damping ratio and synchronism indices that are shown in Equation (2.15) to evaluate power system stability.

2.4 Case Study of Two-Area Power System Small Signal Stability

The two-area power system is presented in [5], and the single line diagram of this system is shown in Figure 2.3 [5]. The system's base is 100 MVA, 230 kV. In order to illustrate the steady state before small disturbance occurs and the state after the small disturbance occurs, the two states are explained using this system. A small disturbance occurs in local mode is applied to the generator #1 and generator #2. The torque of generator #1 is increased by 0.01 p.u. and the torque of generator #2 is decreased by 0.01 p.u. Figure 2.4 presents the speed of the two generators when the disturbance occurs [5].

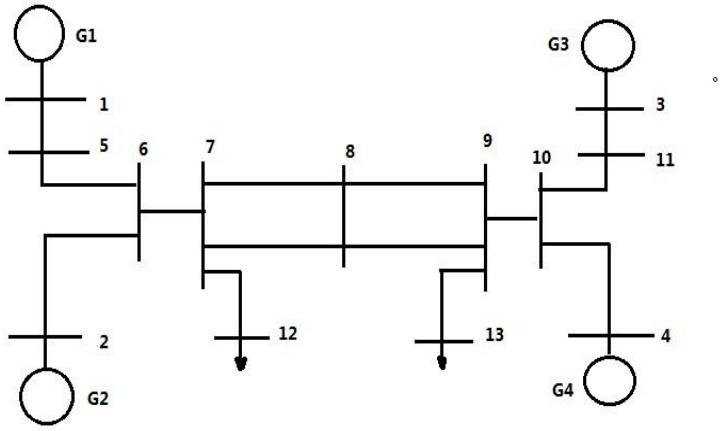

Figure 2.3 Single Line Diagram of Two-Area Power System [5]

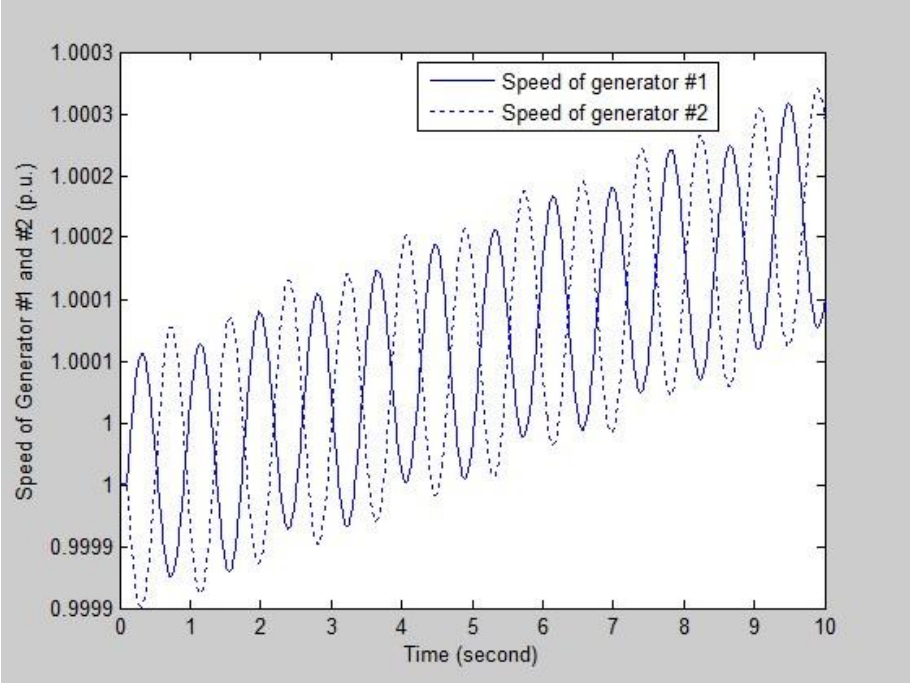

Figure 2.4 Speed of Generator #1 and #2 After the Disturbance

The system is in steady state and with the constant speed of the two generators (G1 and G2) in area one before the disturbance. When the disturbance occurs, the speed of the two generators is oscillating at the frequency of 1.17 Hz [5]. The

oscillations are growing with time increases. The oscillation of speed of generator #2 grows in the antiphase with the oscillation of speed of generator #1. With the growing oscillation, the system becomes unstable. The phenomenon is called small signal stability problem which is caused by small disturbance in power system in a short term. With effective control tools including power system stabilizer and automatic voltage regulator, small signal stability problem can be controlled.

2.5 Conclusion

This chapter provides the overview of the definition of small signal stability problem in power system and the reasons to solve this problem. The model (single generator connected to infinite bus) provides sufficient understanding of how small signal disturbances disrupt the steady-state of power system and the relative component that causes the unstable oscillation. Two-area power system case study which is simulated by Power System Toolbox (PST) [16], illustrates the unstable phenomenon caused by small signal stability and the comparison between steady state and the unstable state.

Chapter 3

Model-Based Analysis for Power System Small Signal Stability

3.1 Introduction

Model-based analysis and measurement-based analysis for power system are two different methods to determine the system's behavior. This thesis will introduce two methods. In chapter 3, model-based analysis is mainly presented. Model-based analysis for power system is based upon the mathematical model of power system, it analyzes power system’s behavior through calculating the eigenvalues of the system’s model. This chapter will introduce the method through case studies.

Section 3.2 will describe the principle of using model-based analysis. The eigenvalue analysis that is commonly used in model-based analysis is introduced in Section 3.2.1. Automatic Voltage Regulator (AVR) will increase the synchronism but it can decrease the damping for power system. The theory of effect after applying AVR is described in Section 3.2.2, the case study in Section 3.2.3 describes this effect. In order to increase damping for power system, power system stabilizer (PSS) is used in power system, the principle is explained in Section 3.2.4 and the case study to

illustrate this effect in shown in Section 3.2.5. Section 3.3 will give the conclusion of this chapter.

3.2 Model-based Analysis

When model-based analysis is used to evaluate the stability of power system, the system can be described as a mathematical model. The property of eigenvalues of the system is used to determine if the system is stable or not. The indices of evaluating the system's eigenvalues includes the polarity, controllability, observability, participation factor, mode shape and sensitivity. Eigenvalue analysis is introduced through case studies in this section.

3.2.1 Eigenvalue Analysis

Assume a nonlinear and dynamic system such as power system, when the system is at equilibrium point, $\dot{x}$ is zero. Therefore, according to Equations (2.1) and (2.5), the system is described as follows:

$$\dot{x}_0 = f(x_0, u_0) = 0 \tag{3.1}$$

$$y_0 = g(x_0, u_0) \tag{3.2}$$

Where x_0 and u_0 refer to the state and input at the equilibrium point, y_0 indicates the output at the equilibrium point. The value of x could be assumed as the change at the state x_0. The relation is described as below:

$$\dot{x} = \dot{x}_0 + \dot{\Delta x} \tag{3.3}$$

Δx is the change at the state of x_0 when disturbance happens. Equation (3.1) is

expressed in this way:

$$\dot{x} = f[(x_0 + \Delta x), (u_0 + \Delta u)] \tag{3.4}$$

Then Taylor's series expansion can be used if the disturbance is small such as small signal stability. Equation (3.4) is expanded as:

$$\begin{aligned} \dot{x}_n &= \dot{x}_{n-0} + \dot{\Delta x}_n \\ &= f_n(x_0 + \Delta x), (u_0 + \Delta u)] \\ &= f_n(x_0, u_0) + \frac{\partial f_n}{\partial x_1}\Delta x_1 + ... + \frac{\partial f_n}{\partial x_m}\Delta x_m + \frac{\partial f_n}{\partial u_1}\Delta u_1 + ... + \frac{\partial f_n}{\partial u_q}\Delta u_q \end{aligned} \tag{3.5}$$

$\dot{x}_{n-0}$ in Equation (3.5) is the derivation state at n th time which is zero, so

$$\begin{aligned} \dot{x}_n &= \dot{\Delta x}_n \\ &= \frac{\partial f_n}{\partial x_1}\Delta x_1 + ... + \frac{\partial f_n}{\partial x_m}\Delta x_m + \frac{\partial f_n}{\partial u_1}\Delta u_1 + ... + \frac{\partial f_n}{\partial u_q}\Delta u_q \end{aligned} \tag{3.6}$$

Similarly, the output can be obtained in the same way:

$$\Delta y_m = \frac{\partial g_m}{\partial x_1}\Delta x_1 + ... + \frac{\partial g_m}{\partial x_m}\Delta x_m + \frac{\partial g_m}{\partial u_1}\Delta u_1 + ... + \frac{\partial g_m}{\partial u_q}\Delta u_q \tag{3.7}$$

To summarize the structures of Equation (3.6) and (3.7), they are expressed as;

$$\dot{\Delta x} = A\Delta x + B\Delta u \tag{3.8}$$

$$\dot{\Delta y} = C\Delta x + D\Delta u \tag{3.9}$$

Where $A = \begin{bmatrix} \frac{\partial f_1}{\partial x_1} ... \frac{\partial f_1}{\partial x_m} \\ ... \\ \frac{\partial f_m}{\partial x_1} ... \frac{\partial f_m}{\partial x_m} \end{bmatrix}$, $B = \begin{bmatrix} \frac{\partial f_1}{\partial u_1} ... \frac{\partial f_1}{\partial u_q} \\ ... \\ \frac{\partial f_m}{\partial u_1} ... \frac{\partial f_m}{\partial u_q} \end{bmatrix}$, $C = \begin{bmatrix} \frac{\partial g_1}{\partial x_1} ... \frac{\partial g_1}{\partial x_m} \\ ... \\ \frac{\partial g_m}{\partial x_1} ... \frac{\partial g_m}{\partial x_m} \end{bmatrix}$ and

$D = \begin{bmatrix} \frac{\partial g_1}{\partial u_1} \cdots \frac{\partial g_1}{\partial u_q} \\ \cdots \\ \frac{\partial g_m}{\partial u_1} \cdots \frac{\partial g_m}{\partial u_q} \end{bmatrix}$. The whole process of calculation is called linearization around small disturbance of power system.

In order to get eigenvalues, the process of lineaization is necessary. The characteristic equation can be obtained from Equation (3.8):

$$\det(A - \lambda I) = 0 \tag{3.10}$$

Where λ is the eigenvalues of matrix A. The value of λ usually represents the stability of a system. Based on the knowledge in control system [2], when

- $\lambda < 0$, the system is stable.
- $\lambda = 0$, the system is at critical position.
- $\lambda > 0$, the system is not stable at all.

However, in power system, the eigenvalues are usually not real, they contain imaginary part. When

- Eigenvalues are real, the negative value stands for decaying oscillation which is the stable state. The positive value means the instability of the system.
- Eigenvalues are conjugate, the real part of eigenvalue represents damping magnitude, when it is positive, the system is stable. The imaginary part provides the frequency of oscillations[6].

3.2.2 Model-Based Analysis of Systems with Automatic Voltage Regulator

As load increases in power system since 1920s, engineers started to focus on

power system stability problem, especially the large interconnected systems and long distance transmission system. Excitation system in synchronous generators is one of the most important elements to effect the stability in power systems during the disturbances. Excitation systems are defined by " An excitation system is the source of field current for excitation of a principal electric machine, including means for its control" [6]. Thus, the principle of excitation systems is to control the direct current of synchronous machine field winding. Two basic functions of excitation systems are protection and control. Protection refers to the function to limit the inputs and outputs in the machines in power system by setting the minimum and maximum values in excitation systems. Control means using excitation system to control the voltage and reactive power in the system [3].

Four elements are used in excitation systems: regulator, exciter, terminal voltage transducer, power system stabilizer. Figure 3.1 illustrates the function of an excitation system [3, 7].

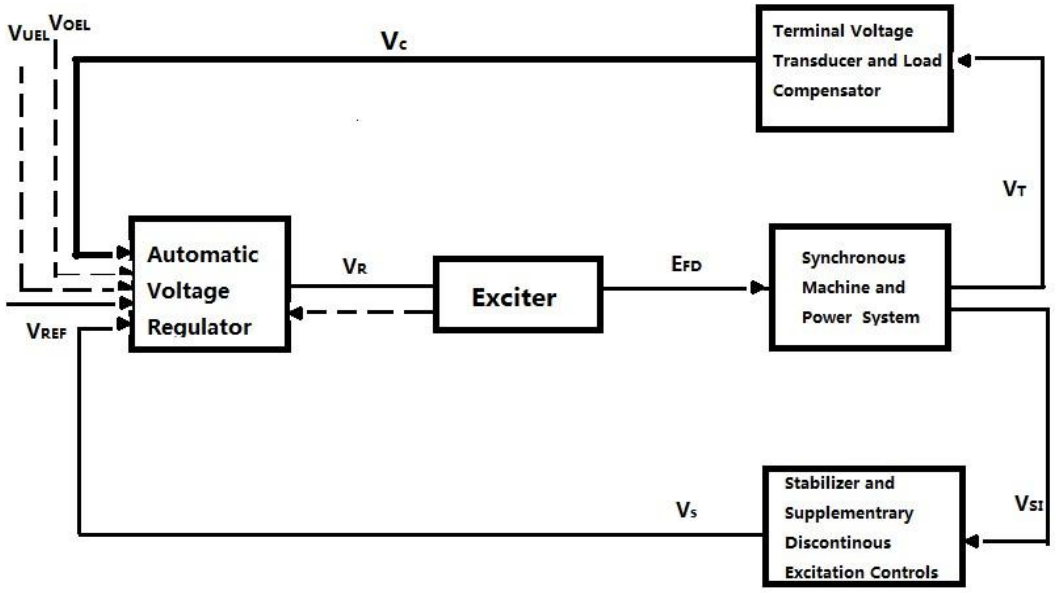

Figure 3.1 General Working Process of Excitation System

The general blocks of excitation systems are the four elements stated above.

- Regulator: make the input signal through a proper way and send to the exciter. It receives the OEL (Over Excitation Limiter) signal (the signal after the over excitation limiter) and UEL (Under Excitation Limiter) signal (the signal after the under excitation limiter).
- Exciter: uses dc power to control the synchronous machine field winding.
- Stabilizer: uses different signals to supply damping to power system oscillations, such as rotor speed deviation.
- Terminal voltage transducer and load compensator: collect the terminal voltage of generator, then transfer to dc values and compare with the desired voltage that set before. Load compensator will use reactive power to compensate in some special situation [3].

Three categories of excitation systems are presented based upon their sources: DC excitation systems, AC excitation systems and static excitation systems. DC excitation systems is driven by DC generators. It controls the rotor of the generator by using the current; AC excitation systems is driven by alternators and the exciter is made on the shaft which the turbine generator stays; static excitation systems refers to the systems that are static, negative voltage signal could be applied to the static excitation systems.

Automatic Voltage Regulator (AVR) will use the generator's terminal voltage to adjust the field voltage in order to control the system's stability. The synchronizing torque coefficient which is caused by the state variable, flux linkages will increase. Therefore, the total synchronizing torque coefficient is increased after applying any types of exciters. By the time, the damping torque component which also caused by flux linkages will become negative values if the gain of exciter is high enough [3]. The higher the gain is, the more negative the damping torque component will be. The oscillations which is caused by the disturbances in the system will become poorly damped but with high synchronizing torque coefficient. This phenomenon is verified by Table 3.1, K_D is decreasing while K_S is increasing.

When adding AVR in the system, the state matrix will change because the whole block diagram is different. The block diagram of the power system is the best way to see the principle of the system and components that will change during the disturbances happens. The block diagram of the system without PSS and amortisseur is shown in Figure 3.2 [3]:

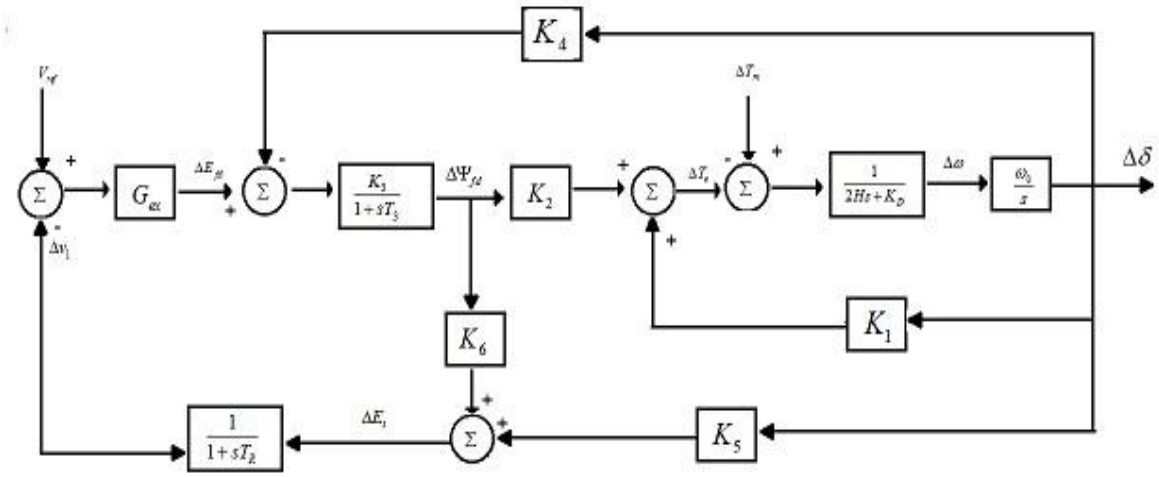

Figure 3.2 Block Diagram of The System With Excitation System [3]

In Figure 3.2, G_{ex} refers to the gain of the exciter, $\frac{1}{1+sT_R}$ is the transfer function of the terminal voltage transducer in the excitation system. In this diagram, the excitation system is chosen to be the thyristor excitation system which is classified as ST1A excitation system. Thyristor excitation system will be used in the case study by given the time constant T_R.

Through the observation of the above block diagram, if one of the state variables changes, the state matrix will become a new matrix. Therefore, the eigenvalues and participation factors are different with the old ones. In Figure 3.2, $K_1, K_2, K_3, K_4, K_5, K_6$ are the constants described like below:

$$K_1 = \frac{V_b E_{q0}}{C}[(X_d'+X_e)\cos\delta_0 + R_e \sin\delta_0] + \frac{V_b I_{q0}}{C}\{(X_q - X_d')[(X_q + X_e)\sin\delta_0 - R_e\cos\delta_0]\} \quad (3.11)$$

$$K_2 = \frac{R_e E_{q0}}{C} + I_{q0}[1 + \frac{(X_q + X_e)(X_q - X_d')}{C}] \quad (3.12)$$

$$K_3 = [1 + \frac{(X_d - X_d')(X_q + X_e)}{C}]^{-1} \quad (3.13)$$

$$K_4 = \frac{V_b}{C}(X_q + X_d')[(X_q + X_e)\sin\delta_0 - R_e\cos\delta_0] \quad (3.14)$$

$$K_5 = \frac{V_{do}}{V_t}X_q[\frac{R_eV_b\sin\delta_0(X_e + X_d')V_b\sin\delta_0}{C}] + \frac{V_{qo}}{V_t}X_d'[\frac{R_eV_b\cos\delta_0 - (X_e + X_q)V_b\sin\delta_0}{C}] \quad (3.15)$$

$$K_6 = \frac{V_{q0}}{V_t}[1 - \frac{X_d'(X_q + X_e)}{C}] + \frac{V_{d0}}{V_t}\frac{X_qR_e}{C} \quad (3.16)$$

Where $C = R_e^2 + (X_e + X_q)(X_e + X_d')$, X_d' is transient reactance, X_e is line reactance, V_{q0}, V_{d0} are the initial values of the generator's terminal voltage on q-axis and d-axis respectively [8]. The participation factors of the state matrix will show the location and reasons that cause the unstable situation.

3.2.3 Case Study of Model Analysis for The Systems With AVR

Consider a thermal generating station has four units of 555MVA, 24 KV for the voltage, the circuit 2 is lost by accident during the process of transmission. This system is an easy system to show the obvious result. Therefore, the lost of circuit 2 should be considered when analyzing the eigenvalues for the system. The plant output is real power equals to 0.9 p.u. and reactive power equals to 0.3 p.u. on the base unit of 2220 MVA and 24 KV. Generator terminal voltage $E_t = 1.0\angle 36^o$, $E_B = 0.995\angle 0^O$. The system diagram is shown in Figure 3.3. Thyristor excitation system is used in this system. The purpose of this case study is to see the effect of adding only AVR [3]. The working process of the thyristor excitation system is shown in Figure 3.4 [3]:

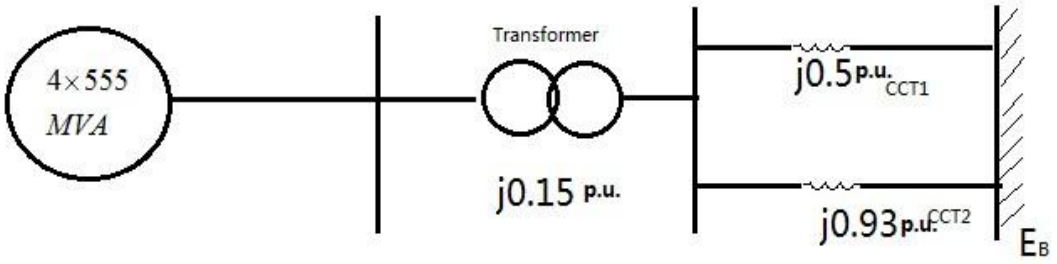

Figure 3.3 Single Line Diagram [3]

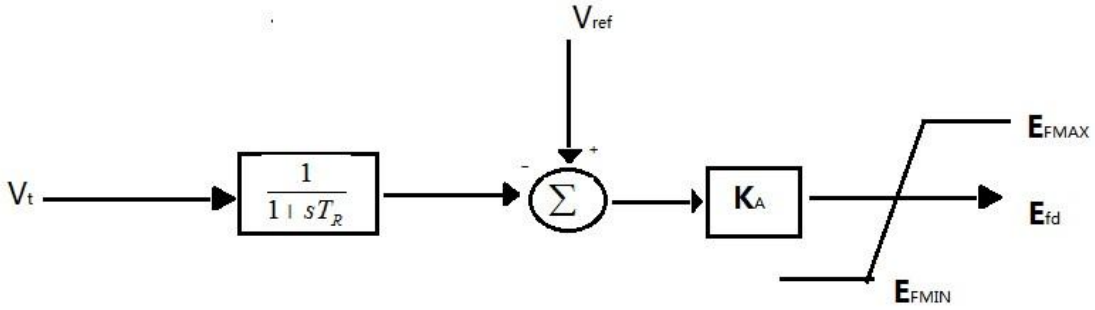

Figure 3.4 Thyristor Excitation System [3]

The state matrix of this system is shown as below:

$$A = \begin{bmatrix} 0 & -0.1092 & -0.1236 & 0 \\ 376.99 & 0 & 0 & 0 \\ 0 & -0.1938 & -0.4229 & -27.3172 \\ 0 & -7.3125 & 20.8392 & -50 \end{bmatrix}$$

As stated in Chapter 2, small signal stability problem should use the eigenvalue to determine the stability when using model-based analysis, the eigenvalues are calculated and shown as follows:

$$\lambda_1 = 0.594 + 7.23i$$
$$\lambda_2 = 0.504 - 7.23i$$
$$\lambda_3 = -20.202$$
$$\lambda_4 = -31.23$$

The eigenvalues of λ_1, λ_2 present the unstable situation of the system because of the positive real parts. In order to analyze which variable is the most influential factor in this system, the participation factor is introduced here to solve this problem.

The state vector Δx as specified in Chapter 2, it is defined as follow:

$$\Delta x(t) = [\ \Phi_1\ \Phi_2\ ...\Phi_n\ ]z(t) \tag{3.17}$$

The vector Φ_n is called right eigenvector, z_t is called the transformed variable and related to the modes. Right eigenvector provides the mode shape for the system. The left eigenvector is defined as the measurement of weighs of the action on the current modes, it is presented as follow:

$$z(t) = [\Psi_1^T\ \Psi_2^T ....\Psi_n^T]^T \Delta x(t) \tag{3.18}$$

The participation factor is created to solve the expression of the relationship and the modes. It combines both right eigenvectors and left eigenvectors. It is shown in Equation (3.19):

$$P_i = \begin{bmatrix} \phi_{1i}\psi_{i1} \\ \phi_{2i}\psi_{i2} \\ ... \\ \phi_{ni}\psi_{in} \end{bmatrix} \tag{3.19}$$

P_{ni} represents the nth state contributes P_{ni} in ith mode. The participation factor according to this case study is shown below:

$$P = \begin{bmatrix} 0.474 & 0.474 & 0.077 & 0.024 \\ 0.474 & 0.474 & 0.077 & 0.024 \\ 0.065 & 0.065 & 2.524 & 1.633 \\ 0.010 & 0.010 & 1.677 & 2.681 \end{bmatrix}$$

The first row's participation factor stands for the speed, the second row's means the rotor angle, the third row's represents the field flux variation, the last row's gives the terminal voltage after the voltage transducer. In order to see which participation factor contributes the most, every row's participation factor should be added up. Therefore, the speed and rotor angle give the highest participation factor after adding them together.

The excitation system without PSS is not efficient because when the gain of the exciter goes larger, the damping of this system will decrease to negative and it will be zero when the gain reaches infinite. To analyze this problem, K_D and K_s are calculated as follows according to this case study and different values of K_D and K_s when the gain of exciter changes.

$$\Delta\psi_{fd} = \frac{-K_3[K_4(1+sT_R)+K_AK_5]}{s^2T_3T_R + s(T_3+T_R)+(1+K_3K_6K_A)}\Delta\delta = \frac{0.988-0.067i}{26.67+17.59i}\Delta\delta$$

$$\Delta T_e = K_2\Delta\psi_{fd} = 0.2115\Delta\delta - 7.06\Delta\omega$$

$$K_s = K_1 + 0.2115 = 0.9758 \text{ pu}$$

$$K_D = -7.06 \text{ pu}$$

In order to show the variation of the damping coefficient, the gain of excitor changes from zero to infinite, all the results are shown in the following table:

Table 3.1 Variation of Damping and Synchronized Coefficient

K_A	K_D	$K_{S\cdot AVR}$	K_S
0	1.1888	-0.004496	0.7598
10	-0.0365	-0.003151	0.761149
15	-0.64133	-0.001139	0.7632
25	-0.18145	0.00314	0.7674
50	-4.343	0.03323	0.7975
100	-7.07	0.1081	0.8724
200	-7.06	0.2115	0.9758
400	-4.645	0.2745	1.0388
1000	-2.0439	0.2988	1.0631
Inf	0	0.3036	1.0679

The results show that the synchronous coefficient is increasing as the gain of exciter increasing, but the damping coefficient is decreasing. This phenomenon illustrates the system lacks of damping and will result in the unstable situation because of lacking damping. To ensure the system operates under stable modes, power system stabilizer must be added in to the system which brings the positive damping to the system [3].

3.2.4 Small Signal Stability Analysis Of Systems With Power System Stabilizer

Power system stabilizer (PSS) uses generator's speed deviation to be the input signal to control the excitation system. As analyzed in the previous section and Table 3.1, when the system adds only AVR without PSS in the excitation system, the gain of the exciter goes up, the damping coefficient drops which results in unstable situation in small signal stability. PSS is installed to solve the problem in the way of adding damping. Three signals can be the input for PSS: the rotor speed, the real power and the bus voltage. In order to create damping to the system, it is connected between the variable ΔE_{fd} and ΔT_e. The phase lag exists between the exciter and electrical torque. PSS also aims to adjust the phase difference here for the exciter. The transfer function of PSS should contain suitable phase compensation circuits to fix the phase lag problem [3].

In order to learn the principle of using PSS to provide damping to the system, the system with no damping is discussed in Equation (3.20):

$$2H\frac{d\omega}{dt} = p_m - p_e \tag{3.20}$$

Equation (3.20) has been clarified in chapter two with damping coefficient. p_e stands for electrical power and it is described as follow:

$$p_e = \frac{E'E_B}{X_T}\sin\delta \tag{3.21}$$

Equation (3.21) is based upon Figure 2.1 in Chapter 2. As p_m is a constant value, when differentiate Equation (3.20), it is shown like below:

$$2Hs\Delta\omega = -\frac{\partial p_e}{\partial \delta}\Delta\delta - \frac{\partial p_e}{\partial E'}\Delta E' - \frac{\partial p_e}{\partial E_B}\Delta E_B \tag{3.22}$$

When the system is stable, E' and E_B are constant. Therefore, the two elements in the differentiating equation (3.22) will become zero. To simplify Equation (3.22) as follow:

$$2Hs\Delta\omega = -k\Delta\delta \tag{3.23}$$

Where $k = \frac{\partial p_e}{\Delta\delta}\Delta\delta$. To unify the variables in above equation, $\Delta\omega = s\Delta\delta$, the equation above will change to the following form:

$$2Hs^2\Delta\delta + k\Delta\delta = 0 \tag{3.24}$$

To analyze the system stability, computing eigenvalues of the above equation is shown below:

$$\lambda_{1,2} = \pm j\sqrt{\frac{k}{2H}} \tag{3.25}$$

PSS aims to add negative part to eigenvalues so that the system could become more stable. Assume $\Delta E_B = k_1\Delta\delta$ since the change of E_B is brought by PSS. Therefore, Equation (3.24) is formed as follows:

$$2Hs\Delta\omega = -k\Delta\delta - k_1\frac{\partial p_e}{\partial E'}s\Delta\delta \tag{3.26}$$

Then the eigenvalues calculated from Equation (3.25) are shown below, bold solid dot refers to the function of multiplying:

$$\lambda_{1,2} = -k_1\frac{\partial p_e}{\partial E' \bullet 4H} \pm j\frac{\sqrt{8kH - (k_1\frac{\partial p_e}{\partial E'})^2}}{4H} \tag{3.27}$$

In this way, the negative real part in eigenvalues are introduced by PSS and the system

is more stable than the one without PSS [9].

There are four blocks contained in PSS diagram: wash-out circuit, phase compensation element, filter, signal limits. Each of them has unique function during the disturbances.

- Filter's function is to optimize the input signal for PSS, eliminate unnecessary disturbances.
- Wash-out circuit aims to reduce steady offset. The time constant in this part could be adjusted to fit the system control.
- Phase compensation element usually contains two blocks and four time constants. The frequencies used for phase compensation is calculated through the four time constants.
- Signal limits is to optimize the output signal. It prevents the output signal causing undesirable saturation in the excitation system [10].

The block diagram for PSS is shown below:

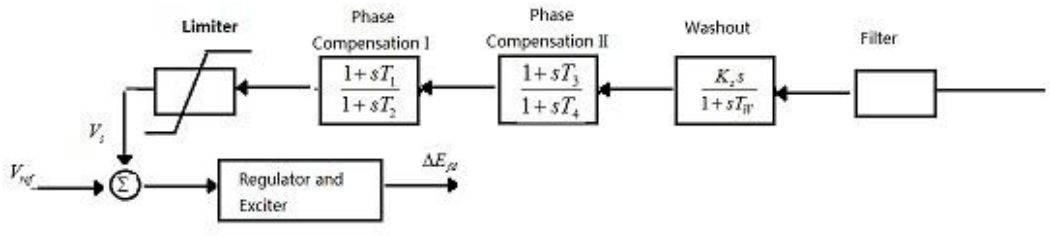

Figure 3.5 Block Diagram of PSS [3]

The system becomes quite different when adding PSS to the diagram as the

oscillation is damped during the small disturbance. The following figure will show the system diagram after adding PSS.

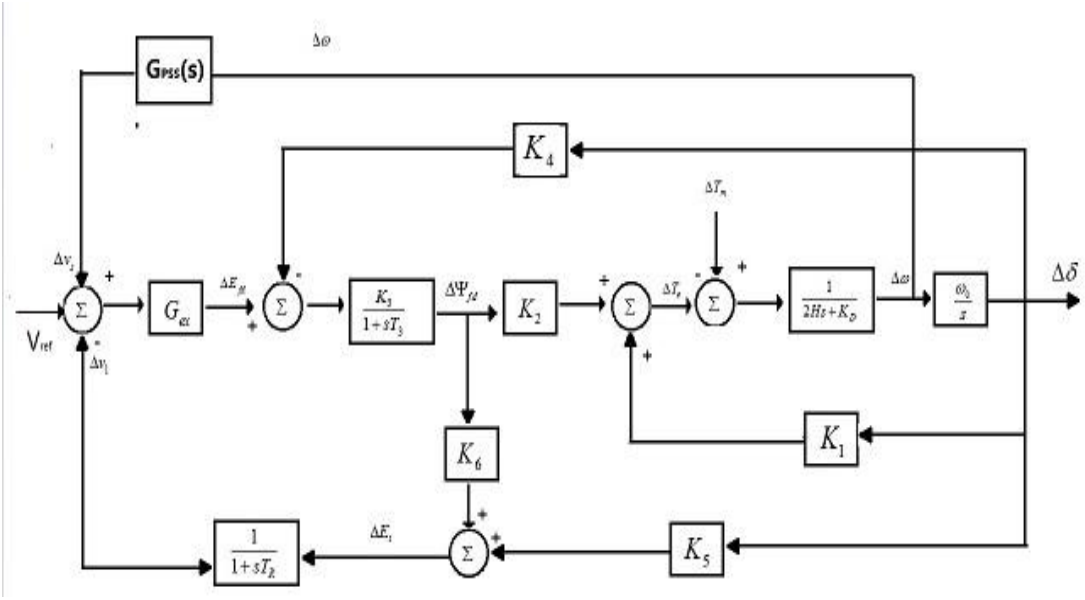

Figure 3.6 Block Diagram of The System With PSS [3]

The state matrix after installing PSS in the system should add the relation about the variable v_s. Assume the gain for power system stabilizer is G_s instead of the filter block. The voltage after the wash-out block is v_2. When use rotor speed to be the input for PSS, then the following equation is obtained:

$$\Delta v_2 = \frac{pT_W}{1+pT_W}(G_s \Delta\omega_r) \tag{3.21}$$

Where T_W is the time constant for wash-out block. In order to make derivation of Δv_2, the following expression is shown based upon Equation (3.21)

$$p\Delta v_2 = a_{51}\Delta\omega_r + a_{52}\Delta\delta + a_{53}\Delta\psi_{fd} + a_{55}\Delta v_2 + \frac{G_s}{2H}\Delta T_m \tag{3.22}$$

Where $a_{51}, a_{52}, a_{53}, a_{55}$ are the coefficients when calculating the state matrix. Therefore, the derivation of output of the change for v_s is obtained as below:

$$pv_s = a_{61}\Delta\omega_r + a_{62}\Delta\delta + a_{63}\Delta\psi_{fd} + a_{64}\Delta v_1 + a_{65}\Delta v_2 + a_{66}\Delta v_5 + \frac{T_1 G_S}{2HT_2}\Delta T_m \quad (3.23)$$

Where $a_{61} - a_{66}$ are the coefficients, T_1, T_2 are the time constants in phase compensate block when assuming only one phase compensate block exists.

State matrix can be obtained in the following form with specified coefficients that relate to different state variables:

$$\begin{bmatrix} \Delta\dot{\omega}_r \\ \Delta\dot{\delta} \\ \Delta\dot{\psi}_{fd} \\ \Delta\dot{v}_1 \\ \Delta\dot{v}_2 \\ \Delta\dot{v}_s \end{bmatrix} = \begin{bmatrix} a_{11} & a_{12} & a_{13} & 0 & 0 & 0 \\ a_{21} & 0 & 0 & 0 & 0 & 0 \\ 0 & a_{32} & a_{33} & a_{34} & 0 & a_{36} \\ 0 & a_{42} & a_{43} & a_{44} & 0 & 0 \\ a_{51} & a_{52} & a_{53} & 0 & a_{55} & 0 \\ a_{61} & a_{62} & a_{63} & 0 & a_{65} & a_{66} \end{bmatrix} \begin{bmatrix} \Delta\omega_r \\ \Delta\delta \\ \Delta\psi_{fd} \\ \Delta v_1 \\ \Delta v_2 \\ \Delta v_s \end{bmatrix} \quad (3.24)$$

All the coefficients can be calculated using the system model [3]. The eigenvalues can be then determined based on the system matrix.

3.2.5 Case Study of Model Analysis for the System with PSS

Consider the 14-Bus power system to present the stability problem. The system is based upon 100 MVA, voltage base for bus 1, 2, 3, 4, 5 is 69 kV, for bus 6, 7, 9, 10, 11, 12, 13, 14 is 13.8 kV, for bus 8 is 18 kV. All the parameters for the system are described in p.u. The load information is described in the Appendix C. All AVR used in this system is the Model One in PSAT toolbox [11]. The system's single line diagram is shown below [12]:

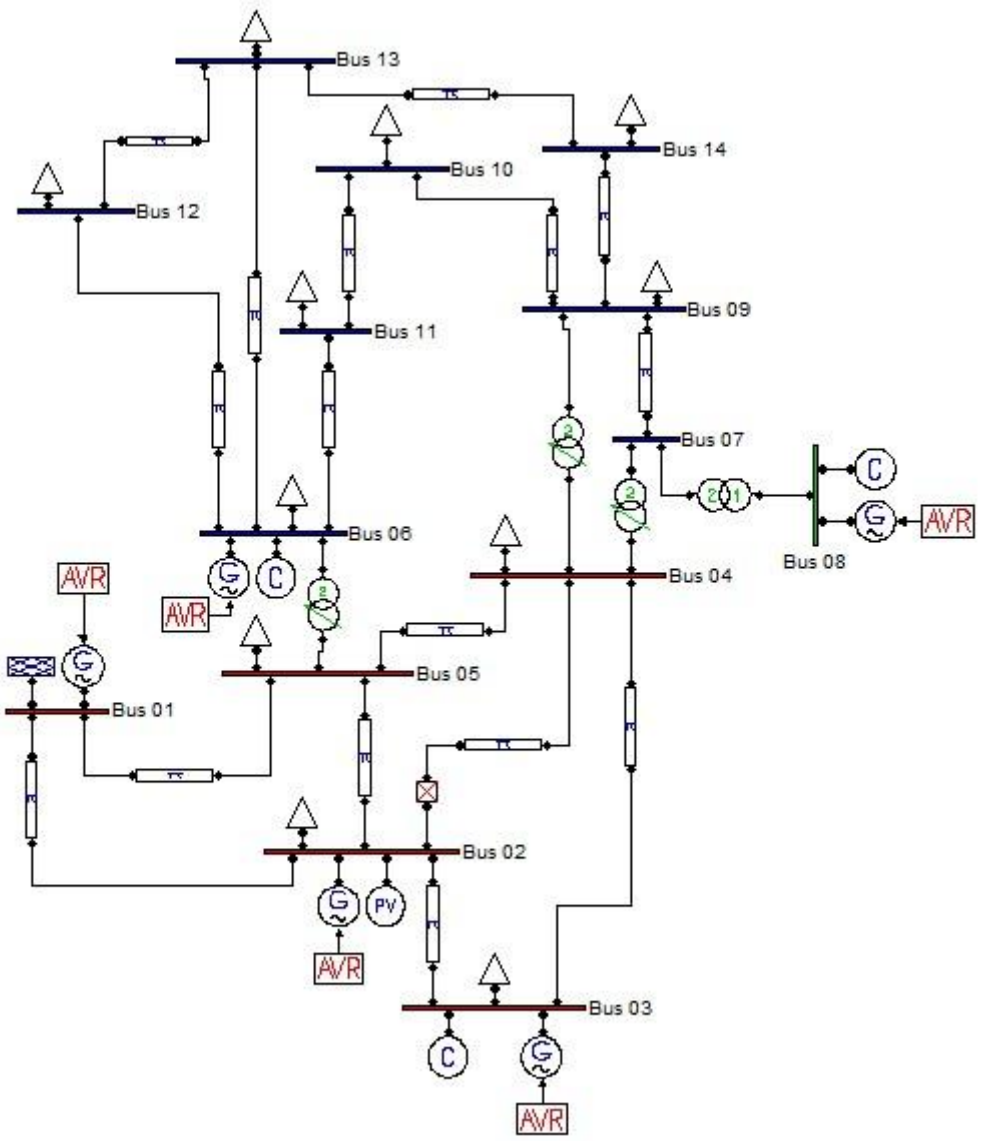

Figure 3.7 Single Line Diagram of IEEE 14-Bus System

In order to learn the property of PSS during real small disturbance, the incidents should be designed to test whether the system is stable or not. Then, the disturbance is designed by increasing the load by 20% in the 14-Bus system with only AVR in the system. The result is shown in Figure 3.8. The eigenvalue property is presented as Figure 3.9:

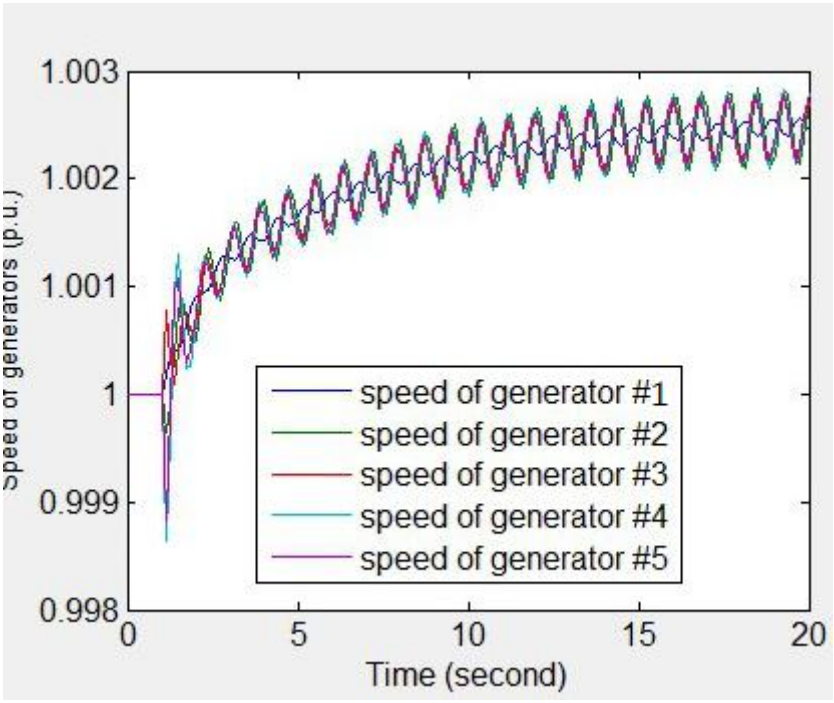

Figure 3.8 Speed of Generators With Disturbance In IEEE 14-Bus System With AVR

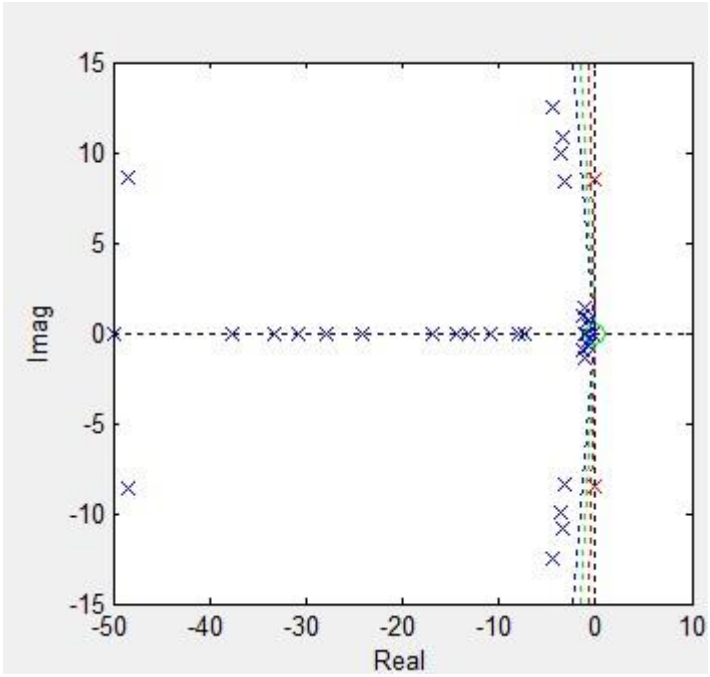

Figure 3.9 Eigenvalues for the 14-Bus system with AVR

The results shown in both Figure 3.8 and 3.9 illustrates an unstable system with

poorly damped oscillation for the rotor speed of generators in the 14-Bus system. Two positive eigenvalues represent the unstable signal to the system. As the disturbance is added to the system, the rotor speed for Generator #1 increases from 1 p.u. to 1.002 p.u.. Power system's state will change if one state changes. The oscillation lacks of damping because of the effect of AVR. The oscillations are in good synchronized mode which is also because of the effect of AVR. The oscillations in Figure 3.8 need to increase the damping to make the system become stable. As analyzed in Table 3.1, damping coefficient will increase if adding PSS to the system. According to the eigenvalues and participation factors' analysis for IEEE 14-Bus, one PSS should be added to Generator #1 [12]. After adding PSS to the system, the rotor speed variation is shown as Figure 3.10. Figure 3.11 describes the eigenvalues for the new system which indicates the stable situation because of all negative terms.

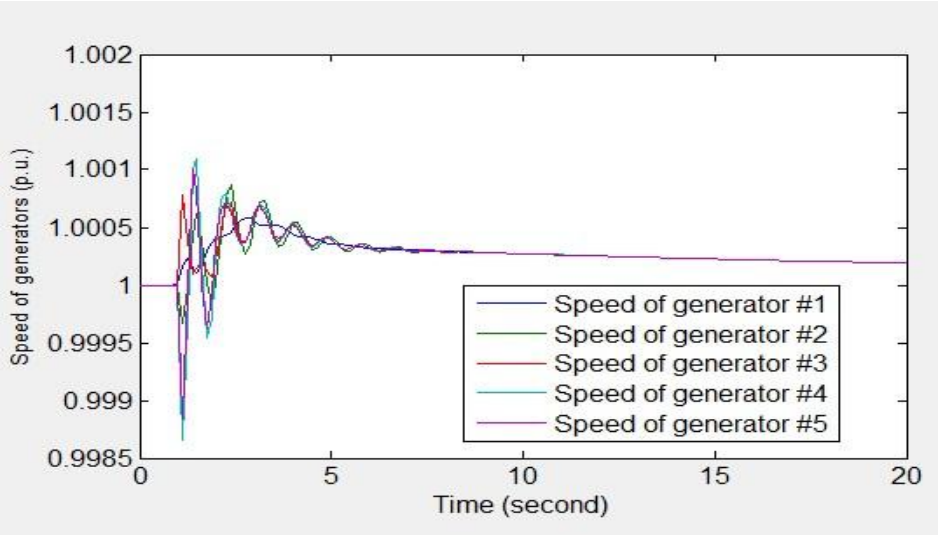

Figure 3.10 Rotor Speed Variation of Generators With Disturbance In IEEE 14-Bus System With PSS

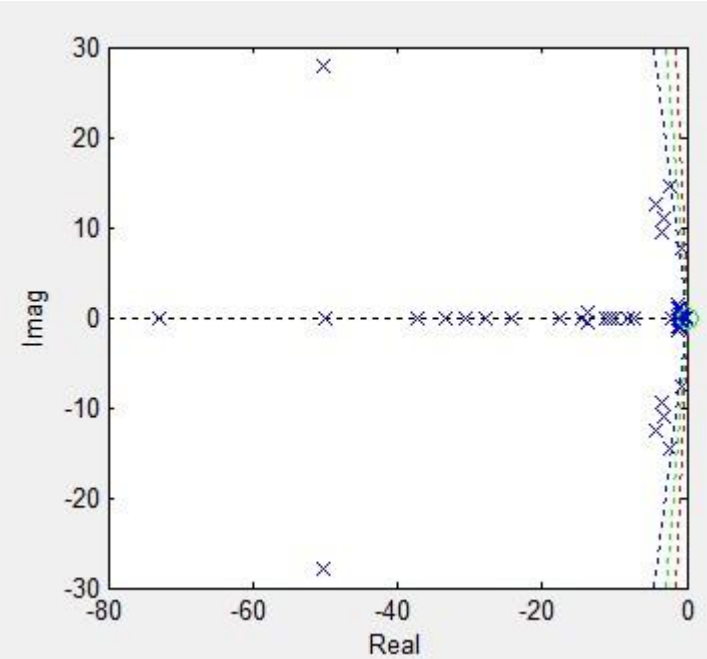

Figure 3.11 Eigenvalues for the 14-Bus system with PSS

The same load disturbance is still applied to the system. For Generator #1, the rotor speed initially is 1 p.u., it first oscillates between one sec. and five sec., then it becomes stable around five sec.. The three generators are operating at 1.00004 p.u.. The system eliminates oscillations for the rotor speed. Damping is added to the oscillation to the system when the disturbance happens. The state of the system changes if the parameters change. The Jacobian Matrix and eigenvalues for the state matrix will be different if adding PSS [14]. Therefore, adding PSS efficiently improves the stability for power systems.

3.3 Conclusion

This chapter describes the principle of using model-based analysis for the system.

The participation factor calculated from the system can be used to see which state relates to the unstable eigenvalues. The reason of adding PSS in the excitation system is illustrated through Table 3.1 which shows the damping coefficient variation with different gain of AVR. The location of adding the PSS can be determined using participation factor [12]. PSS will add damping to the oscillation in the system. The simulation of adding PSS in the 14 bus system in this chapter shows that the system is stable if using PSS in the excitation system. The system lacks of damping because of using only AVR in the excitation system. The eigenvalues in model-based analysis verifies the stable state after adding PSS and unstable state with only AVR in the system.

Chapter 4

Wide - Area Measurement System (WAMS)

4.1 Introduction

Wide - Area Measurements System (WAMS) is deployed in power systems for many years, aiming to increase the efficiency for economic dispatch and stability control for power systems. Originally, power system applies supervisory control and data acquisition (SCADA) system to determine the current state for the system. However, the measurements from SCADA system are not instantly and accurately made [18]. In 1990s, an equipment named Phasor Measurement Unit (PMU) that could estimate the state of power system, including voltage magnitude, current magnitude and the phasors for the both variables was developed. PMUs use synchrophasor measurements to obtain the system's state from the sampled data and are built to form the network which is named WAMS. When analyzing small signal stability problem, the most conventional method is to use the Linearized Differential Algebraic Equation (DAE) based mathematical model to develop eigenvalues and participation factors for the system that being disturbed. However, the process to use this method is very complicated and the mathematical model cannot express precisely

for the dynamic power system [15]. Therefore, a more accurate method - synchrophasor measurement used in PMU to determine the state of power system is needed for the analysis of small signal stability.

In this chapter, the application, principle and structure of PMU are described in Section 4.2 including the method for estimating the state for power systems. The combination of the simulations and the theory used in PMUs is stated in Section 4.3. Section 4.4 gives a case study for applying DFT to obtain phasor for a tested voltage signal. Section 4.5 provides the concluding remarks.

4.2 Phasor Measurement Unit

Phasor Measurement Unit is based upon the synchrophasor measurement from the existing power systems. Synchrophasors are the expression of mathematical method by the phasor values of the sinusoidal waveforms in power system. The measurement derived from the synchrophasor is called synchronized measurement. The state including bus voltage magnitude, line current magnitude, their phase angles and the frequency of power system can be measured directly in this way. Comparing to the former methods to estimate the state of power systems, synchrophasor can obtain the magnitude of the bus voltage, current and their phasors. Before the method of synchronized measurement, bus voltage is commonly used to represent the state of power systems. One of the reasons that causes the popularity of using synchronized measurement is the synchronized function. In order to get the data with the same time stamp from different location, PMUs uses the Global Position System (GPS). Even if

the location is remote, the data from every distributed location can be collected by PMU with the time-stamped real-time measurements at the same time. Synchrophasor measurement can result in fewer errors in convergence and topology than conventional methods. Synchrophasor measurement based PMU provides various useful information during analyzing problems in transient stability, small signal stability and voltage stability [15 - 21].

4.2.1 Principle of Phasor Measurement Unit

The first PMU was built in Virginia in the year of 1990 and made of standard microprocessor systems, analog/digital input cards, a Central Processing Unit (CPU) and interface units [21]. Initially, it focused on the local disturbance records and monitoring for local areas. However, the needs for the computer based relay increase, the state of the whole system should be provided. Therefore, WAMS deploys PMU and Phasor Data Concentrator (PDC) in the system. The measurements from PMU can be either sent to PDC or the local storage space. All the data can be collected from different places by PDC at the same time. The feature assists power systems accurately find out the causes that make the whole system unstable [20]. PMUs are installed on buses. However, one PMU's cost can be from ten thousand dollars to seventy thousands dollars. The detail for the situation of PMUs' installation in some countries is presented in [19]. Although PMU is very effective in determining the state of power systems, it is not necessary to install PMU on every bus. The topic of the positions that are suitable for installing PMU has become a popular research direction

in power system's monitoring. The virtual buses refer to the buses that are not practical to install PMUs, such as the shunt elements nodes, can be eliminated from the install positions. Moreover, based on the unique type of transmission line used in the system, PMU can only be installed on one side of the bus. The method to eliminate the redundant positions to install PMUs is described in [20].

PMU owns the characters of real-time measurements and fast and accurate measurement based on the unique structure. Figure 4.1 shows the basic architecture of the PMU [19].

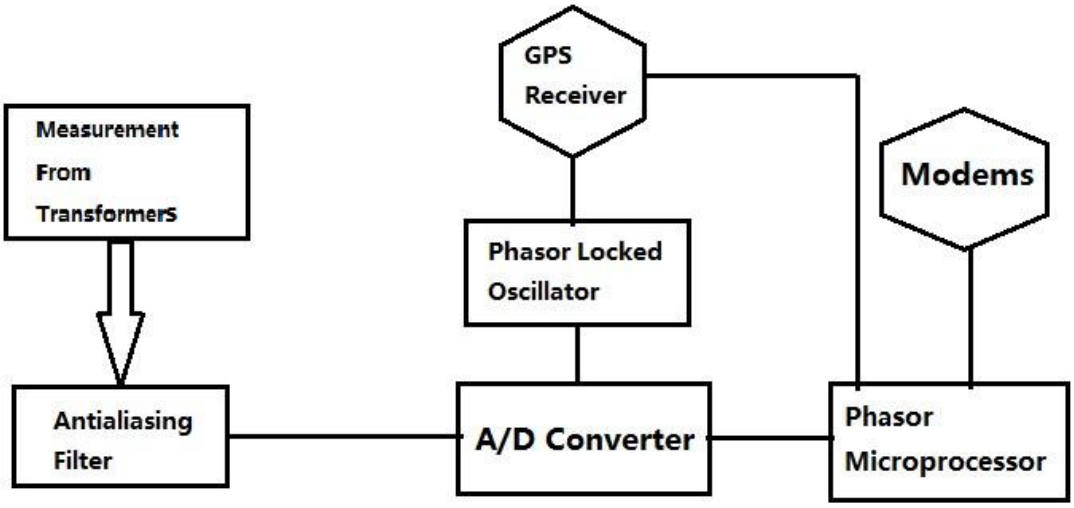

Figure 4.1 Basic Architecture of Phasor Measurement Unit [19]

Each PMU consists an anti-aliasing filter, GPS receiver, phasor locked oscillator, analog to digital converter and phasor microprocessor. The sampling times of the measurements including currents and voltage from the secondary windings of the current and voltage transformers could be twelve times per cycle at the early stage, but now it increases to ninety-six or one hundred and twenty-eight times per cycle [17]. The function of each element is described as follows:

- Anti-aliasing filter aims to prevent the samples from measurements from aliasing. During sampling from measurements, if the sampling's frequency is not more than two times of the analyzed signals' frequency, the signals in a specific zone will overlap, and then the samples become errors. The phenomenon is called aliasing. Anti-aliasing filter is to avoid the errors during sampling by satisfying Nyquist criterion [17].
- A/D converter is the equipment that converts the data from anti-aliasing filter to digital signal that can be used by the phasor micro-processor.
- GPS receiver could collect the signal that is sent by GPS. GPS has the unique function of sending out ceaseless and rhythmic time signal by one pulse per second [17]. GPS receiver could be low-cost equipment and the signal sent by GPS is not able to be interrupted by electrical noise [21].
- Phasor-locked oscillator is the equipment that controls the sampling intervals and it is phase-locked with GPS clock pulse. It could check the time automatically. Recently, the sampling rate has been increased, and it has the trend to go higher because of the accuracy when analyzing the state of systems [17].
- Phasor micro-processor uses the specific algorithm to calculate the state. The algorithms for this part have been developed for different categories. Next section will introduce the most common algorithm applied in PMU to estimate phasors for the system. Three sorts of data from PMU are restored and sent: system disturbance type data which is the measurement collected immediately after the

disturbance, such as line tripping; ambient type measurement which is measured under normal systems; data from direct dynamic tests of the system to determine the specific condition that the system is in [15, 17]. Finally, the data from PMU is sent to higher hierarchical equipment to be collected through the modem.

4.2.2 Application of PMUs

Phasor measurement unit has been applied to different area in power system since it was developed in early stage. It provides real-time and accurate data for power system, and the data is very useful for improving power system control and protection. With installing distributed PMUs, power system control and protection will not only rely on local data. Table 4.1 shows the application of PMUs in power system [15, 20, 25, 26, 28, 34].

Table 4.1 Application of PMUs in Power System [15, 20, 25, 26, 28, 34]

Application to	Purpose
Power System Monitoring	Postevent monitoring
	Digital system disturbance recorders (DSDRs)
	State estimation for WAMS
Power System Protection	Improve control and backup relay performance
	Adaptive out-of-step protection
	Power swing protection using system integrity protection schemes
	Improve security-dependability
Power System Control	Control based on measurement value of remote quantities
Voltage Stability	Estimates voltage stability index
Small Signal Stability	Estimates damping, frequency and mode shape of poorly damped oscillatory modes
Transient Stability	Estimates phase angles deviation, potential and kinetic energies of synchronous machines
	compare with the instability's thresholds

The main purpose of PMUs is the state estimation. Before the introduction of PMUs, the state cannot be determined directly. In addition, the previous methods cannot collect the state of the system in synchronization, including power flows, net power injections and voltage and current magnitudes [24]. PMU brings the real-time direct measurements without assuming the system is static. By installing PMU at the most optimal points will make the system more efficient [11]. Because of deploying the unique estimation method, the state of power systems (bus voltage, current, phase angles and frequency) are obtained directly through sampled data and DFT method in PMUs. The combination of GPS in PMUs makes synchronization becomes reality which means to get the measurements at the same time from all the PMUs [20].

Supervisory Control And Data Acquisition (SCADA) system is commonly used in monitoring the state of power systems. However, the rate of measurements from SCADA system is much lower than PMU's. Therefore, the more accurate and speedy measurements from PMU should support for the SCADA system to monitor the whole system. The application that includes PMU and SCADA system in WAMS is shown in Figure 4.2.

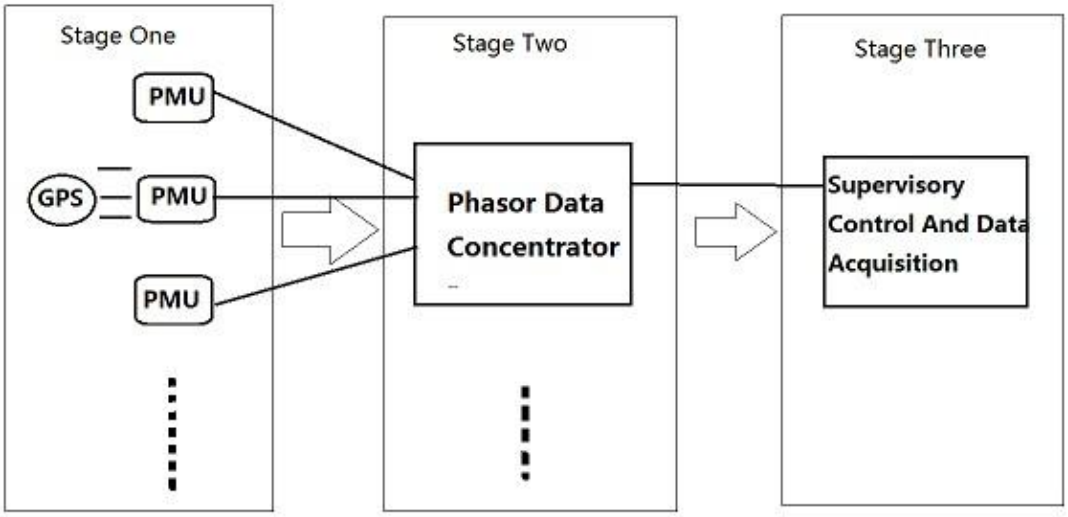

Figure 4.2 Application of PMUs in WAMS [17, 22]

PMU's application is the first stage to monitor the system's state. With the constant support from GPS, PMUs collect the phasor and magnitude of the current and voltage from each substation, then the data is sent to PDC through high quality communication links. Phasor Data Concentrator aims to collect the data from every PMU, abandon the bad data, using the unique time-stamped function from data to summarize the data that collected at the same time. Not only one PDC is deployed in

the power system. All the data gathered from PDC is then sent to the SCADA system to support a more accurate system's estimation [17, 22].

4.2.3 Estimation in PMUs

Phasor Measurement Unit uses the sampled data to estimate the phasor of the voltage and current. However, phasor representation can only be extracted from pure sinusoidal wave. In power system, the signal contains the signal at different frequencies. One method used to extract the waveform at signal frequency is to use Fourier transform. The most popular method applied in PMU is to use Discrete Fourier Transform to estimate phasor representation in power systems [17].

To define phasor representation of a sinusoidal signal, the signal described as $x(t)$ is shown below:

$$x(t) = X_m \cos(\omega t + \phi) \tag{4.1}$$

Where ϕ is the phase angle in the unit of radians. X_m is the peak value of the signal. The phasor representation of the above signal is shown as [9]:

$$X = (X_m / \sqrt{2}) e^{j\phi} \tag{4.2}$$

Figure 4.3 gives a pure sinusoidal signal and Figure 4.4 shows the phasor representation of a pure sinusoid signal [17].

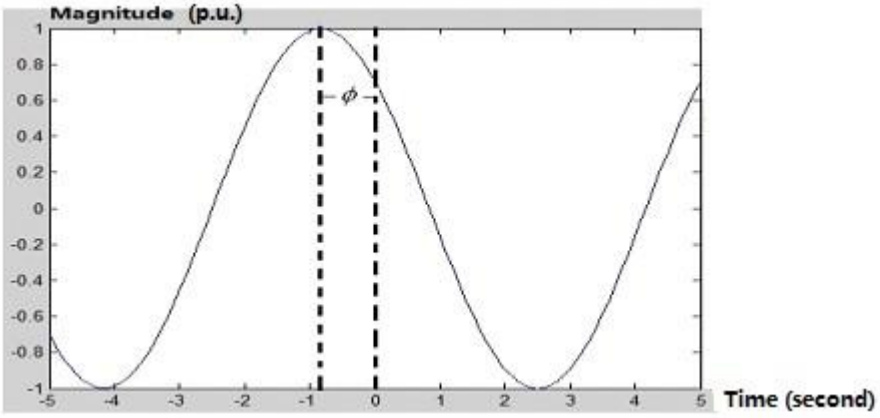

Figure 4.3 Expression of Pure Sinusoidal Signal In The Time Scale

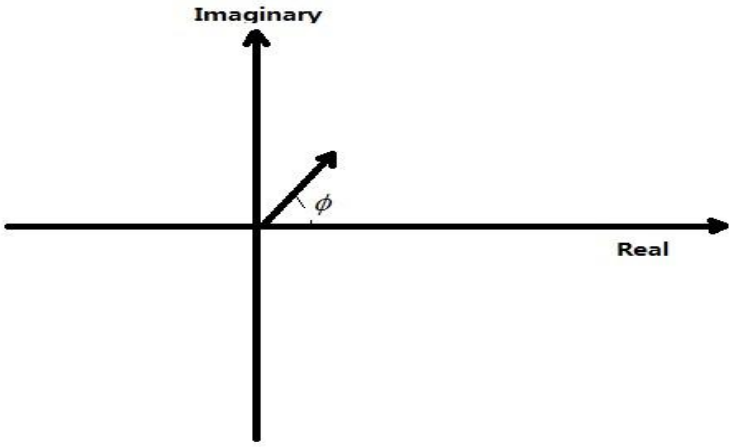

Figure 4.4 Phasor Expression of Pure Sinusoidal Signal

Discrete Fourier Transform (DFT) is the most commonly used method in PMUs. By using discrete steps through a finite window in frequency domain to complete Fourier Transform. Suppose a signal $x(t)$ that is shown in Equation 4.3 is sampled at the sampling angle $\theta = 2\pi / N$, N is the the number of samples during one finite window.

$$x(t) = a_k \cos(2\pi k f_0 t) + b_k \sin(2\pi k f_0 t) \tag{4.3}$$

Where a_k, b_k are the Fourier series coefficients. Because of the periodic property of

DFT, the coefficients of Fourier series can be obtained through the sampling data. The k th component's phasor representation is obtained below:

$$X_k = \frac{1}{\sqrt{2}} \frac{2}{N} \sum_{n=0}^{N-1} x(n\Delta T) e^{-\frac{j2\pi kn}{N}} \tag{4.4}$$

Where n represents the nth sample, because the values are the same when the frequencies are $\pm nf_0$, ΔT is the time length per window for sampling, the multiplier two should exists in Equation (4.4). To describe the above equation in the form of sine and cosine, Equation (4.5) is presented like below:

$$X_k = \frac{\sqrt{2}}{N} \sum_{n}^{N-1} x\ (n\Delta T)[\cos(kn\theta) - j\sin(kn\theta)] \tag{4.5}$$

Usually, the above equation is expressed as Equation (4.6):

$$X_k = X_{kc} - jX_{ks} \tag{4.6}$$

Where X_{kc}, X_{ks} represent for the cosine component and the sine component [17, 23].

New phasor needs to be calculated using the algorithm provided above. Two methods are developed to determine the new phasor: Nonrecursive updates and recursive updates. Nonrecursive updates is the most easy way to estimate new phasor. Every estimation will repeat all the process through N samples. One window could estimate one phasor, the next phasor will use the the samples from the next window. The next estimation stage uses the repeated N-1 samples from the previous window and one new sample to calculate the new phasor. The sample windows is shown in Figure 4.5. In this way, the phasor estimation becomes very stable because the new estimation process would not use the previous samples [17]. However, the

computation needs lots of space.

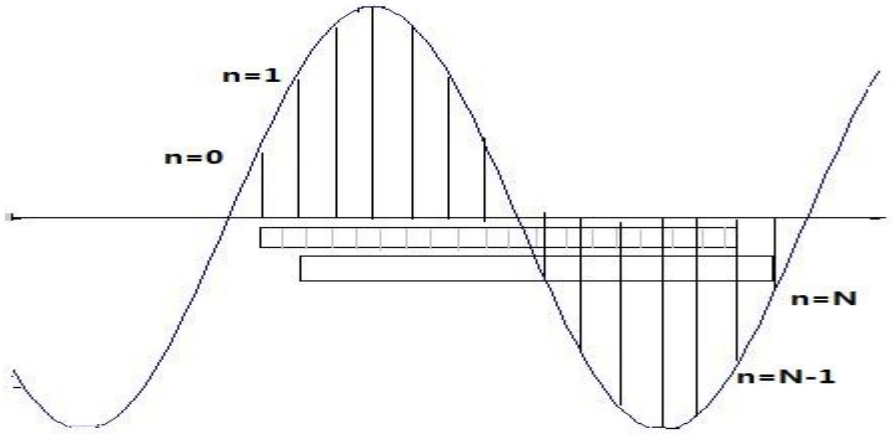

Figure 4.5 Sample Windows For Phasor Estimation In DFT

Recursive updates method is more faster and uses less space during the computation. Therefore, the computation process will be less trouble if using the estimation in the previous window. Recursive updates method saves lots of space during estimation. However, its estimation process is easily affected by one error from samples because of the recursive property. Recursive updates method is now the most common method for estimation phasor [17, 23].

4.3 Case Study of Signal Estimation

Suppose a signal is described as below:

$$x(t) = 8 + 15 \times \cos(377t + 30 \bullet \pi / 180) + 6 \bullet \cos(2 \times 377t + 45 \bullet \pi / 180) + 2 \bullet \cos(377t + 60 \bullet \pi / 180)$$

The fundamental frequency is 60 Hz. The length of one window is 16.66 ms. The samples are collected 100 times per window. The purpose of this case study is to use

Discrete Fourier Transform (DFT) to estimate this signal. As DFT is used for periodic signal, so Fourier Series Coefficients can be used to represent the the signal's value. Based on the value calculated by DFT, the Fourier Series Coefficients are obtained. First ten coefficients are determined by DFT method for this signal. The results calculated by DFT with 100 samples per window are shown in Table 4.2.

Table 4.2 Discrete Fourier Transform of 100 Samples in One Window [17]

Frequency	0	f_0	$2f_0$	$3f_0$	$4f_0$ ~(-6 f_0)
DFT/100	8.0042	6.4949 - 3.7549i	2.1182 - 2.1234i	0.4973 - 0.8652i	0
Frequency	-5 f_0	-4 f_0	-3 f_0	-2 f_0	- f_0
DFT/100	0	0	0.4973 + 0.8652i	2.1182 + 2.1234i	6.4949 + 3.7549i

Since time domain analysis cannot provides the full information of signals with different frequencies. DFT uses samples to estimate based on the frequency domain. The sampled signal is expressed by Discrete Fourier Transform method in the frequency domain and also in time domain in Figure 4.6:

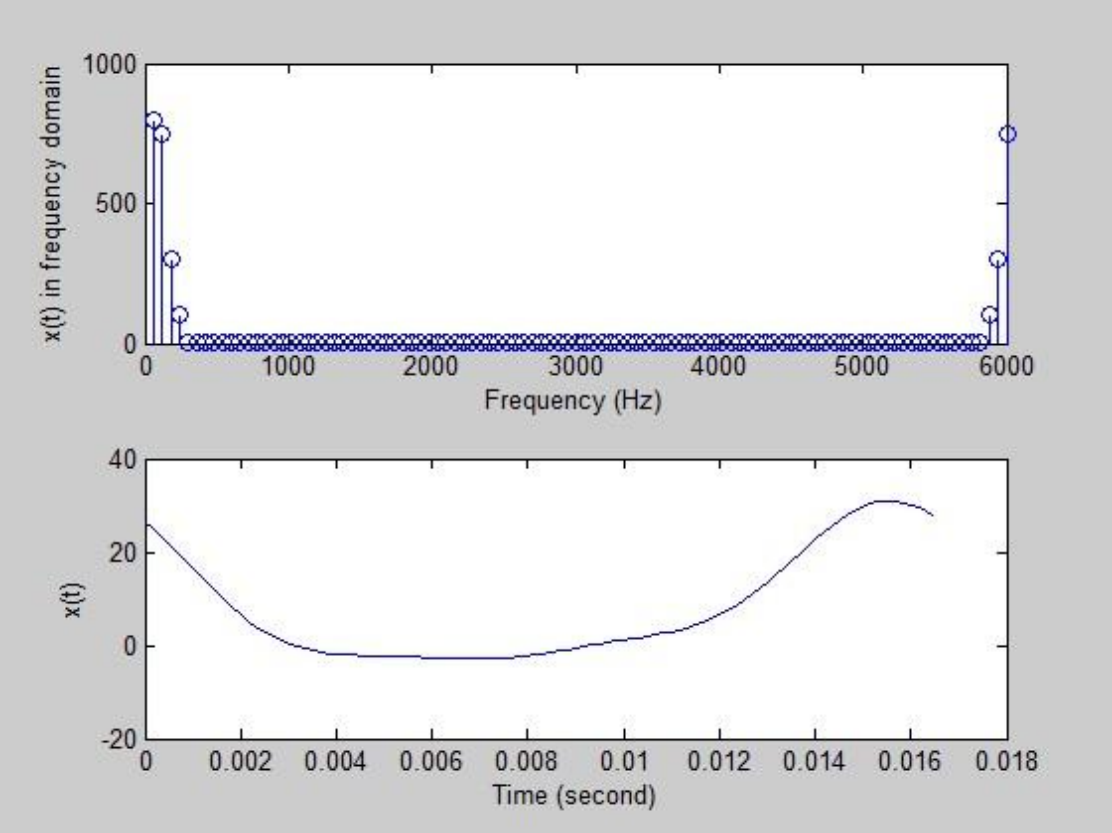

Figure 4.6 Expression of the Signal in Both Frequency Domain and Time Domain

Figure 4.6 shows the transformation of the signal from time domain to the frequency domain. In order to see the significance of using DFT to estimate the signal, it is necessary to compare the difference between the results of the estimation and the actual signal. The Fourier Series Coefficients are calculated as below:

$$a_0 = 2 \times 8.0042/2 = 8.0042$$

$$a_1 = 2 \times 6.4949 = 12.9898$$

$$b_1 = 2 \times (-3.7549) = -7.5098$$

$$a_2 = 2 \times 2.1182 = 4.2364$$

$$b_2 = 2 \times (-2.1234) = -4.2468$$

$$a_3 = 2 \times 0.4973 = 0.9946$$

$$b_3 = 2 \times (-0.8652) = -1.7304$$

The signal estimated based on the 100 samples in one window can be expressed with Fourier Series Coefficients as below:

$$f(t) = 8.0042 + 12.9898\cos(377t) - 7.5098\sin(377t) + 4.2364\cos(2 \times 377t) - 4.2468\sin(2 \times 377t) + 0.9946\cos(3 \times 377t) - 1.7304\sin(3 \times 377t)$$

The expansion of the original signal is described as follow:

$$f(t) = 8 + 12.99045\cos(377t) - 7.5\sin(377t) + 4.243\cos(2 \times 377t) - 4.243\sin(2 \times 377t) + \cos(3 \times 377t) - 1.732\sin(3 \times 377t)$$

The comparison of the original signal and the estimated signal is shown below:

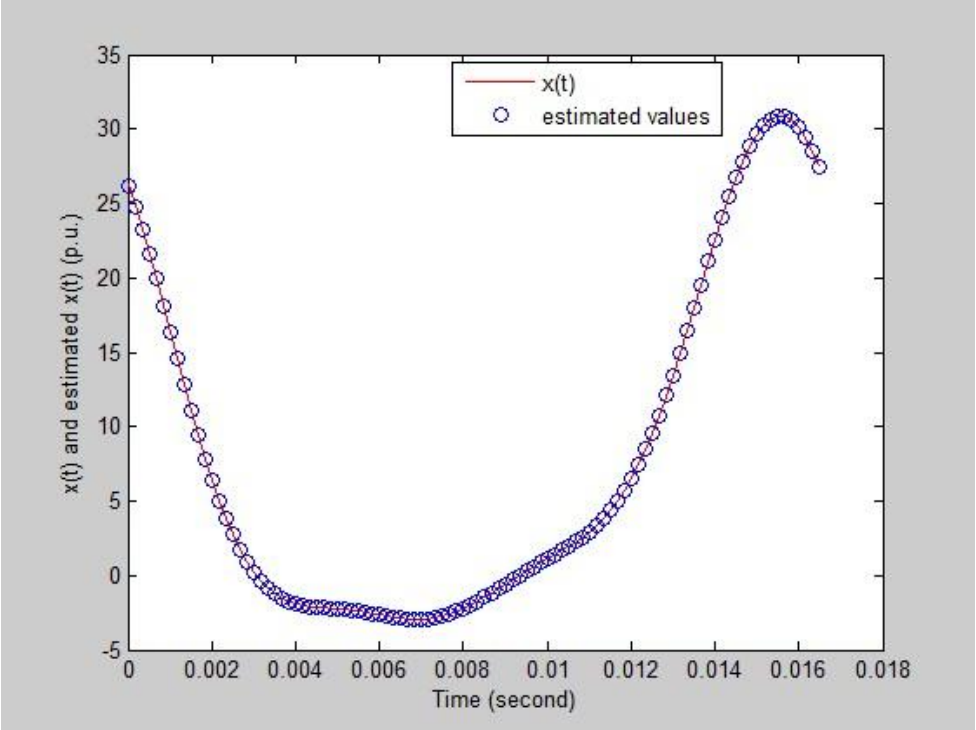

Figure 4.7 Comparison of The Original Signal and The Estimated Signal

Figure 4.7 illustrates the proficiency of using DFT to estimate the signal, the circle in the figure presents the estimated value, the line stands for the actual value of the signal in the time domain. From the expressions between the Fourier Series Coefficient and the original signal could tells the benefit of using DFT method. The estimated values are almost the same as the actual value and fit the original values. Using Fourier Series Coefficients to estimate the signal is efficient also because of the periodic property which saves lots of space when calculating. The accuracy of DFT method makes it become one of the most popular solution to measure the power system's state. PMUs use DFT method to estimate the voltage and current magnitude and their phase angles. All the measurements from PMUs are collected with the time stamped characteristic at the same time from the system. The accurate measurements through DFT method improve the stability analysis of power system.

4.4 Case Study of Applying DFT to Obtain Phasor

Consider a bus voltage signal which is provided to the system of 60 Hz. The signal is expressed as $x(t) = 100\cos(120\pi t + \pi/4)$. The sampling rate is at 24 samples every cycle. The case study will apply the DFT get the phasor. The sampling angle is $2\pi/24$. By using recursive phasor estimation method, the phasor of this signal is shown in Table 4.3 [17]. The magnitude of this signal is 70.7 kV. Based on the relationship between DFT and Fourier Series, the phasor of the signal is calculated based on the following equation:

$$X = \frac{\sqrt{2}}{N}\sum_{n}^{N-1} x\ (n\Delta T)[\cos(kn\theta) - j\sin(kn\theta)] \qquad (4.7)$$

Table 4.3 Phasor of Voltage Signal With Non-recursive Phasor Estimation

Number	0	*23*	*24*	*25*	*26*
Sample	*70.7107*	*86.6025*	*70.7107*	*50*	*25.8819*
Phasor	*/*	*/*	$70.7107\angle 45$	$70.7107\angle 60$	$70.7107\angle 75$
Number	*27*	*28*	*29*	*30*	*31*
Sample	3.0616×10^{-14}	*-25.8819*	*50*	*-70.7107*	*-86.6025*
Phasor	$70.7107\angle 90$	$70.7107\angle 105$	$70.7107\angle 120$	$70.7107\angle 135$	$70.7107\angle 150$

As non-recursive phasor estimates the signal is operated by certain sampling angle, for this case study is $\pi/12$. Therefore, there is additional 15 degree for every estimation. As the magnitude for this signal is constant, the estimation gives constant magnitude for this signal. The phasor fits the original signal.

4.5 Conclusion

This chapter presents the purpose of Wide-area Measurement System in power system and the significance of applying PMUs to power systems. In order to describe the method that is used in PMUs to obtain the instant measurements of the state in power systems, including voltage, current magnitude and their phase angles and frequency, the numerical case studies provide the principle to estimate signals using

DFT method and to get the phasors for the signal. The results of the case studies show the proficiency of using DFT to estimate signals. PMUs have been widely used in power system to get instant measurements of the system's state. Therefore, the introduction of applications for PMUs in power system indicates the meaningful improvements for power system analysis. Snychrophasor technology used in distributed installed PMUs can be applied to monitor wide-area power system small signal stability.

Chapter 5

Measurement-Based Analysis for Power System Small Signal Stability

5.1 Introduction

Measurement-based analysis is a real-time monitoring method for power system. It is different from model-based analysis, it uses PMUs to obtain the information for power system. Measurement-based analysis provides accurate data and predict of the stability behavior based on synchrophasor technology in Chapter 4.

After the incidents of Western Interconnection and Eastern Interconnection [1], large power system should be visualized using wide-area synchronized measurements. Interconnected power system is more complex, it needs large computing space and better algorithm to realize the visualization. Based on wide-area synchronized measurement, many tools have been developed for monitoring power system, such as Synchronized Measurement and Analysis in Real Time (SMART ®) tool, RTDMS software and AREVA T&D's e-terra*vision* ™ [27].

The fundamental purpose of using wide-area measurement is to determine the

system's oscillation and damping. Small signal disturbance happens in low frequency among one or a group of generators swing against another group of generator. The undamped oscillation can cause blackout. Two methods are used to determine the oscillation property. One is oscillation detection, the identification is completed within several seconds after the the oscillation become intensive. The other one is mode meter, it can predict the damping for the power oscillation and provide the early detection of the mode for oscillations. Prony method can predict the mode for power oscillations [27].

In this chapter, measurement-based analysis is introduced and applied to a large power system: 68-bus power system [5]. In order to present the visualized character, a small disturbance is designed during the simulation. Measurement-based analysis is introduced in Section 5.2. Section 5.2.1 illustrates the principle of applying prony method to the measurements collected from PMU. Section 5.2.2 uses the two-area power system to demonstrate the measurement-based analysis for this power system. Section 5.3 gives the 68-bus power system, 39-bus power system and the tools to study in this power system. Section 5.4 presents case studies for the interconnected power systems, including the the phasors estimated in the system using DFT recursive method, the real-time power flow in the system and the analysis of oscillation using prony method. Section 5.5 gives the deployment of measurement-based analysis in power system. Section 5.6 concludes this chapter.

5.2 Measurement-Based Analysis

When analyzing power system stability, the most common method is to use the eigenvalue analysis to determine the eigenvalues for power systems based on the model characteristic. The method needs to linearize the model that is formed by the differential and algebraic equations around only one equilibrium point. However, system's operation point is not the same all the time. Hence, the real-time condition for power system is not easy to capture using model-based analysis.

Synchrophasor measurements are precisely obtained from PMUs to determine the instantaneous state of power system. The measurement-based analysis for small signal stability can be used for predicting the power system's behavior including voltage, current and frequency using the synchrophasor measurements from PMUs. Compared to Supervisory Control and Data Acquisition (SCADA) systems, PMU has much higher frequency for collecting samples. Synchrophasor measurements are provided with time stamp to view the entire interconnected power system. In order to determine the oscillation property of the system, prony analysis is used to estimate the damping ratio, frequency and mode shape of poorly damped electromechanical oscillations that are needed to see the trend of oscillations [15].

5.2.1 Principle of Prony Method

The method discussed for measurement-based analysis is to use the PMUs installed in power system buses to obtain the state of the system. This includes voltage,

current magnitude and their phasors and the frequency. Prony method is then applied to the measurements from PMUs. The damping ratio, frequency and mode shape of the oscillation are determined by this step. Prony method is a viable method to model linear system which contains damped complex exponentials to uniformly sampled signals. The information provided by prony method is useful for analysis of the stability of the power system.

Suppose the signal collected from PMUs is expressed as Equation (5.1):

$$\hat{y}(t) = \sum_{i=1}^{L} A_i e^{(\sigma_i t)} \cos(2\pi f_i t + \phi_i) \tag{5.1}$$

where Ai refers to the amplitude of component i, σ_i is the damping coefficient of component i, ϕ_i is the phase of component i, f_i is the frequency for component i, L is the total number of damped exponential components, $\hat{y}(t)$ is the estimated value for $y(t)$. $y(t)$ can be the real power, voltage magnitude or current magnitude. Prony method provides visual information directly using the principle described below.

Equation (5.1) could be expressed as Equation (5.2) when $t = K * T$ and $\cos(2\pi f_i + \phi_i) = \frac{e^{j(2\pi f_i + \phi_i)} e^{j\phi_i}}{2} + \frac{e^{-j(2\pi f_i + \phi_i)} e^{-j\phi_i}}{2}$, T is the time length per sampling window

$$y[k] = \sum_{i=1}^{L} C_i \mu_i^k \tag{5.2}$$

Where $C_i = \frac{A_i}{2} e^{j\phi_i}, \mu_i = e^{(\sigma_i + j2\pi f_i)T}$ the two coefficients: C_i and μ_i contains the information to analyze the system's behavior, such as the frequency and damping ratio. Prony method aims to obtain these two components. Equation (5.2) is shown in matrix

form in Equation (5.3） as below:

$$\begin{bmatrix} y[0] \\ y[1] \\ .. \\ . \\ . \\ y[N-1] \end{bmatrix} = \begin{bmatrix} 1 & 1 \\ \mu_1^1 & \mu_L^1 \\ \mu_1^2 & .. \mu_L^2 \\ .. & .. \\ \mu_1^{N-1} & \mu_L^{N-1} \end{bmatrix} \begin{bmatrix} C_1 \\ C_2 \\ C_3 \\ ... \\ C_L \end{bmatrix} \tag{5.3}$$

Assume that μ_i is the root of nth order polynomial with unknown coefficients a_i which is shown below:

$$\mu^L - a_1\mu^{L-1} - ... - a_{L-1}\mu - a_L = 0 \tag{5.4}$$

After transformation for Equation (5.4), the signal is expressed with the formation of the current measurements and the previous measurements with unknown coefficients ai as follow:

$$\begin{bmatrix} y[L] \\ y[L+1] \\ .. \\ . \\ . \\ y[N-1] \end{bmatrix} = \begin{bmatrix} y[L-1] & y[L-2] & .. & .. & y[0] \\ y[L] & y[L-1] & .. & .. & y[1] \\ y[L+1] & y[L] & .. & .. & y[2] \\ .. & .. & .. & .. & .. \\ y[N-2] & y[N-3] & .. & .. & y[N-L-1] \end{bmatrix} \begin{bmatrix} a_1 \\ a_2 \\ a_3 \\ .. \\ a_L \end{bmatrix} \tag{5.5}$$

To conclude the steps for calculating damping ratio and frequency using prony analysis, first using Equation (5.5) to obtain the 'a' vector because other information in Equation (5.5) is the measurements. Second, compute the roots of 'a', since 'a' is known, the coefficient μ_i can be get directly. Finally, the coefficient 'C' from Equation (5.2) could be calculated [15]. The information obtained from the three steps is used to understand the stability of the power system. The following case study is used to illustrate the application of the method.

5.2.2 Case Study of Measurement-Based Analysis for Two-Area System

The case study assumes PMUs are located in the two-area system. The system installs three PMUs at Bus 4, 7 and 9. The placement for PMUs are calculated using Graph theoretic procedure installed in PSAT toolbox based on Matlab [13]. Then the real-time measurement of the voltage magnitude is collected by PMU. In order to test the efficient of using prony method, a small disturbance of increasing 0.01 p.u. for the torque of the generator one and decreasing 0.01 p.u. for the torque of generator two is set to complete a time domain simulation. The nominal frequency is 60 Hz. The bus magnitude for bus 7 and 9 is shown below [5, 13]:

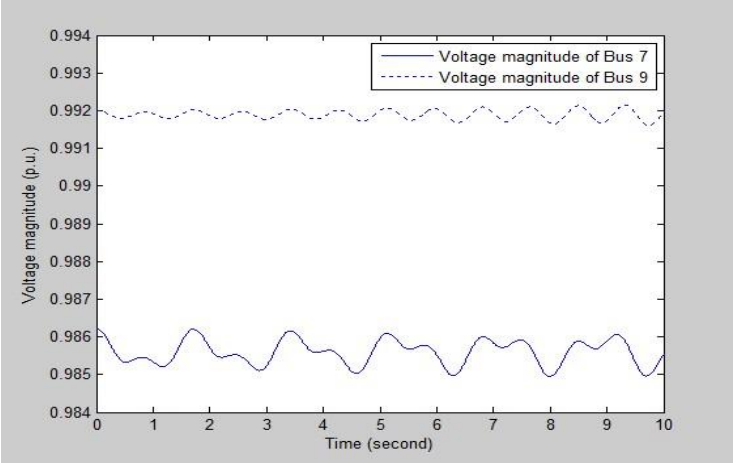

Figure 5.1 Voltage Magnitude of Bus #7 and #9 in Two-Area System

The simulation starts from zero second and lasts for 10 seconds. The voltages for bus seven and nine in the system lacks of damping, so the system is in the unstable situation. Eigenvalues analysis is usually applied to determine the oscillation property

using participation factors and eigenvalues. However, the thesis uses prony method to detect the frequency and damping ratio of the system. Figure 5.2 provides the prony estimation of the voltage magnitude of bus seven.

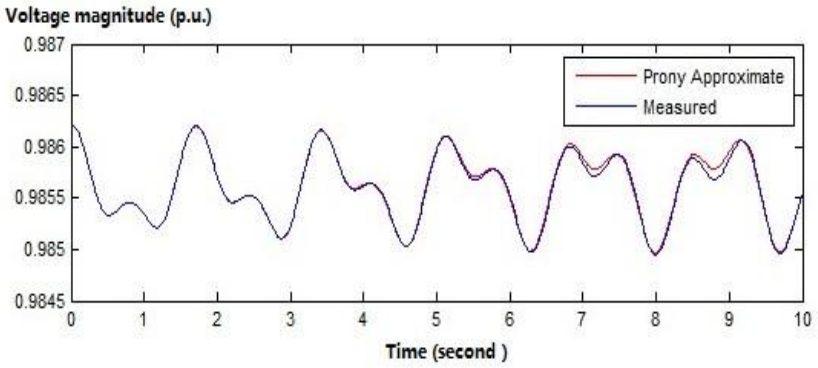

Figure 5.2 Prony Estimation for Voltage Magnitude at Bus #7

The result shown in Figure 5.2 verifies the efficiency of using prony method to estimate the state of power system. The estimated values fit the original values with small difference. The damping ratio and frequency could be provided accurately based on the nice estimation from prony method. The system's operation is a continuous process, PMUs could offer continuous real-time synchrophasor measurements which accurately present the state of power system. Prony method uses the effective measurements from PMUs, then provides the damping coefficients for the two-area system's voltage magnitude which is shown below:

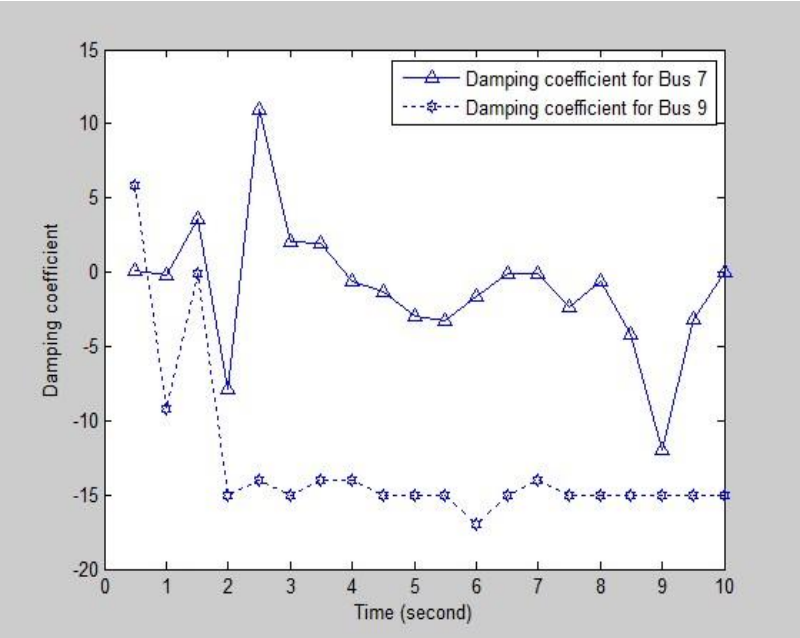

Figure 5.3 Damping Coefficient Detected by Prony Method

Damping coefficients shown from Figure 5.3 verifies the oscillation's property. The damping coefficients are almost negative which results in the undamped oscillation for the system. In addition, most of the damping coefficients for bus nine is close to each other which indicates the oscillation magnitudes increase with same changes. The damping coefficient reflects the nature of the oscillation. The trend of the oscillation could then be determined with the information provided by prony method.

5.3 Test Systems and Tools for Study

5.3.1 68-Bus Power System

The 68-bus power system is used in Chapter 5. The single line diagram is shown in Figure 5.4 [5]. There are 68 buses and 86 lines in this system. The system is based on 100 MVA [29]. Graph theoretic method is used to compute the placement of PMUs. The placement of PMU is preferred to the most connected bus. There are totally 20 PMUs needed in this system based on this algorithm. The placement of PMUs in 68-bus power system is shown in Table 5.1 [12, 30, 33].

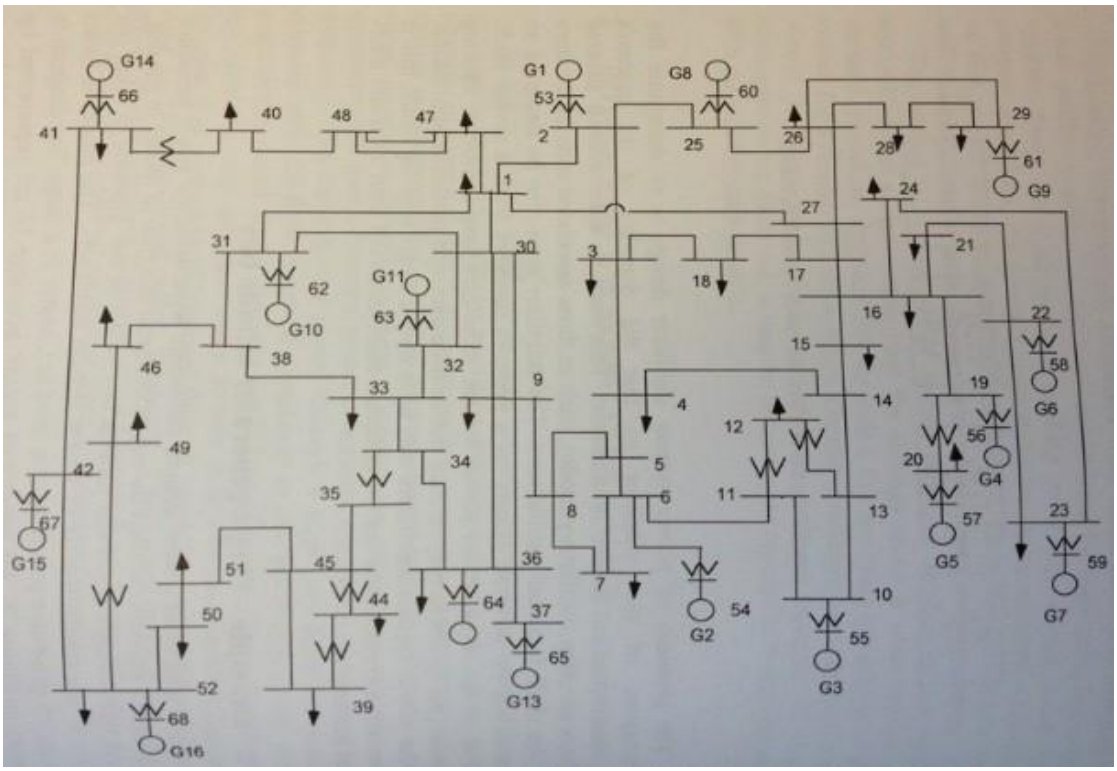

Figure 5.4 Single Line Diagram of 68-Bus Power System [5]

Table 5.1 PMUs' Placement for 68-bus Power System

Buses	68
Lines	86
PMUs	20
Location	Bus 2, 6, 10,14,16, 20, 23, 26, 30, 36, 38, 41, 43, 45, 48, 52, 60, 61, 65, 67

5.3.2 39-Bus Power System

New England 39-bus power system is tested in this chapter. The system's single line diagram is shown in figure 5.5 [35, 36]. The system has three areas, namely Area 1, 2, 3. The system contains ten generators and 39 buses. Area 1 includes the bus 1, 2, 3, 17, 18, 25, 26, 27, 28, 29, 30, 37, 38. Area 2 includes bus 4, 5, 6, 7, 8, 9, 10, 11, 12, 13, 14, 31, 32, 39. Area 3 has bus 15, 16, 19, 20, 21, 22, 23, 24, 33, 34, 35, 36. The system is based on 100 MVA, 60 Hz and 100 kV. The system has 20 load buses. The total generation is 6192.84 MW and the load is 6150.1MW. Graph theoretic method is also used to compute the placement of PMUs in this power system. The locations for PMUs in 39-bus power system are shown in Table 5.2 [12].

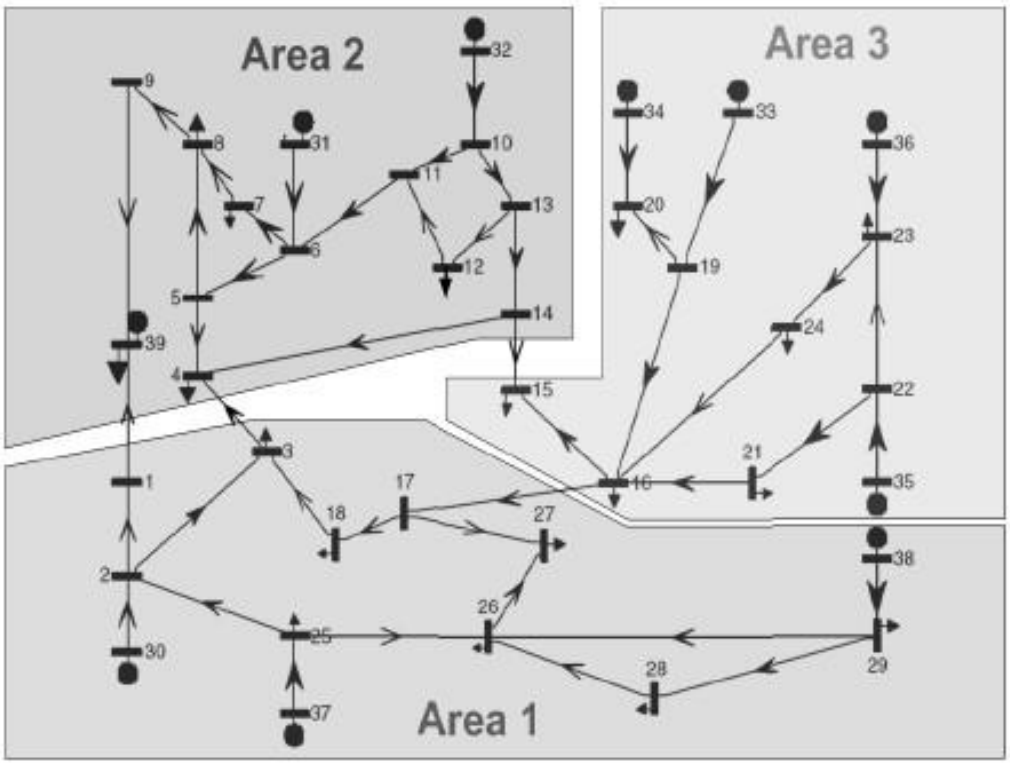

Figure 5.5 Single Line Diagram for 39-Bus Power System [35, 36]

Table 5.2 PMUs' Placement for 39-bus Power System

Buses	39
Lines	46
PMUs	11
Location	Bus 2, 6, 9, 10, 14, 16, 20, 23, 26, 37, 38

5.2.3 Tools for Study

The software used in this chapter is based on Matlab. Basically, the tools are the toolboxes applied in Matlab. Power System Toolbox (PST) is used to simulate 68-bus

power system and 39-bus power system. Power System Analysis Toolbox (PSAT) provides the calculation of PMUs' placement. Prony Toolbox is used for the mode analysis of power oscillation in 68-bus power system and 39-bus power system. These toolboxes support the case studies in this chapter.

5.3 Case Studies

When analyzing power system's small signal stability using wide-area measurement, the phasor of bus voltages, line current and the magnitude of voltages, line current and power flow in the whole system are the indicators for stability. In this section, these indicators are simulated for 68-bus power system. The mode of oscillation is then estimated by prony method and provided to the operator. For the 39-bus power system, the inter-area oscillations are presented by the bus voltages. The frequency and damping are shown in this case study according to the inter-area oscillations.

5.3.1 Measurement-based analysis for 68-bus power system

A. Phasor of Bus Voltages and Line Current

In this section, the phasor of bus voltages that are affected by the disturbance is discussed as well as the bus voltage magnitude. In order to learn the changes of phasor, a disturbance is created during the simulation. The mechanical torque of synchronous generator one is decreased by 0.01 at 0.1 second. PST is used in this section. The system's base frequency is 60 Hz, it is a 100 MW based power system. The detail for

this system is present in Appendix D.

Figure 5.6 gives the variation of phasor of Bus 1, 2, 18, 47, 48. The phasor is calculated by recursive method based on DFT. The phasor of Bus 1, 2, 18, 47, 48 oscillates after 0.1 second because of the disturbance of decreasing 0.01 p.u. for generator one's mechanical torque. The oscillation of phasor shown in Figure 5.6 indicates that the damping should be negative at first few seconds. Then the oscillation gradually becomes less oscillated, which indicates that the damping is increasing. When using wide-area synchrophasor measurement to analyze power system's stability, the mode is provided to verify this phenomenon. Figure 5.7 shows the phasor of voltage for Bus 2, the oscillation become intense after 0.1 second. Bus voltages also become unstable for few seconds. The sampling rate to get phasors is 24 samples per cycle. Figure 5.8 gives voltage magnitude for Bus 2. When the system is stable (before the disturbance), the voltage magnitude at Bus 2 is maintained at 1.046 p.u., it starts oscillate after the disturbance is applied, the oscillation is decreasing after around 5 seconds. The whole oscillation is not in a large amplitude range, the largest magnitude of voltage at Bus 2 is 1.0464. Line current magnitude is also shown in Figure 5.9, the current at first is stable at 0.76 p.u.. The disturbance enables the oscillation of line current. The oscillation frequency is higher for the line current.

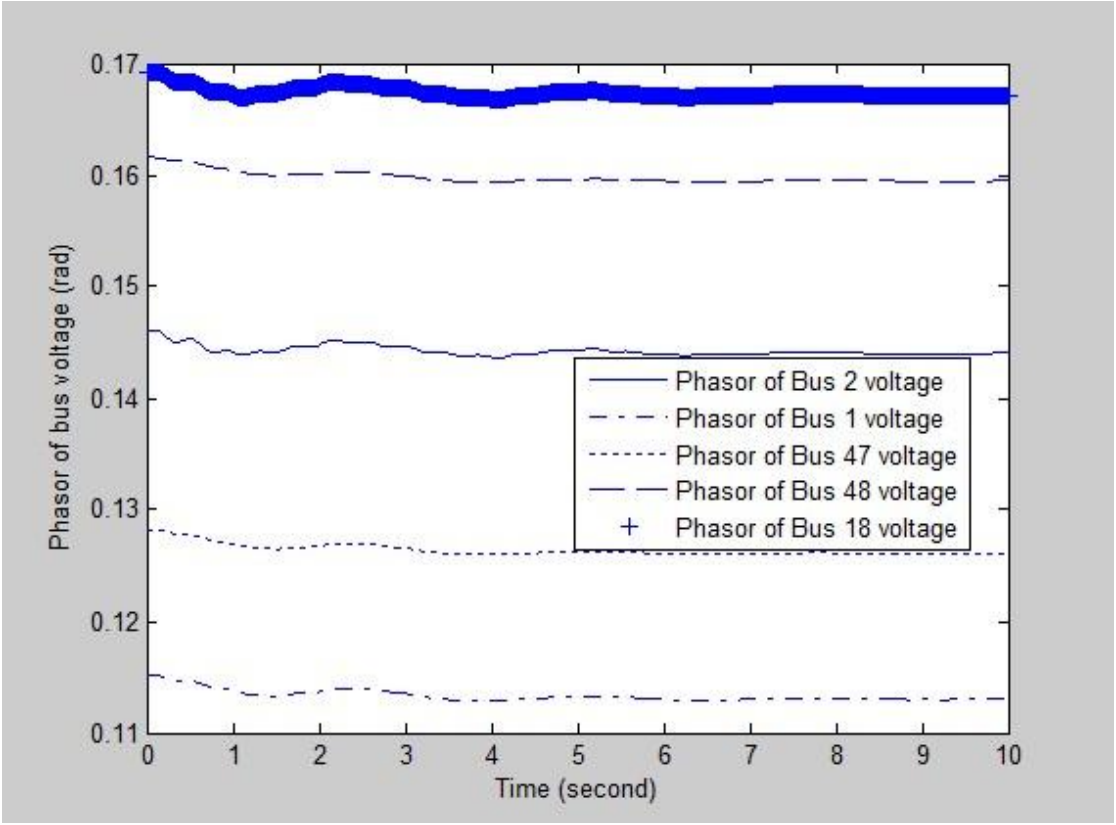

Figure 5.6 Phasor Variation of Voltages for Bus 1, 2, 18, 47, 48

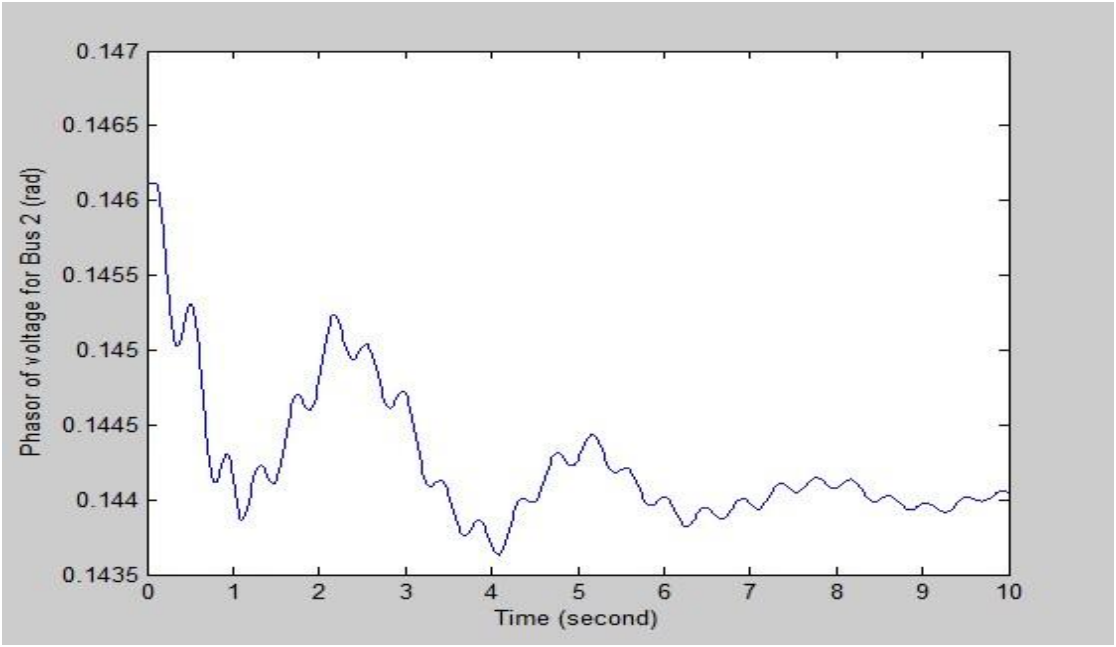

Figure 5.7 Phasor of Voltage for Bus 2

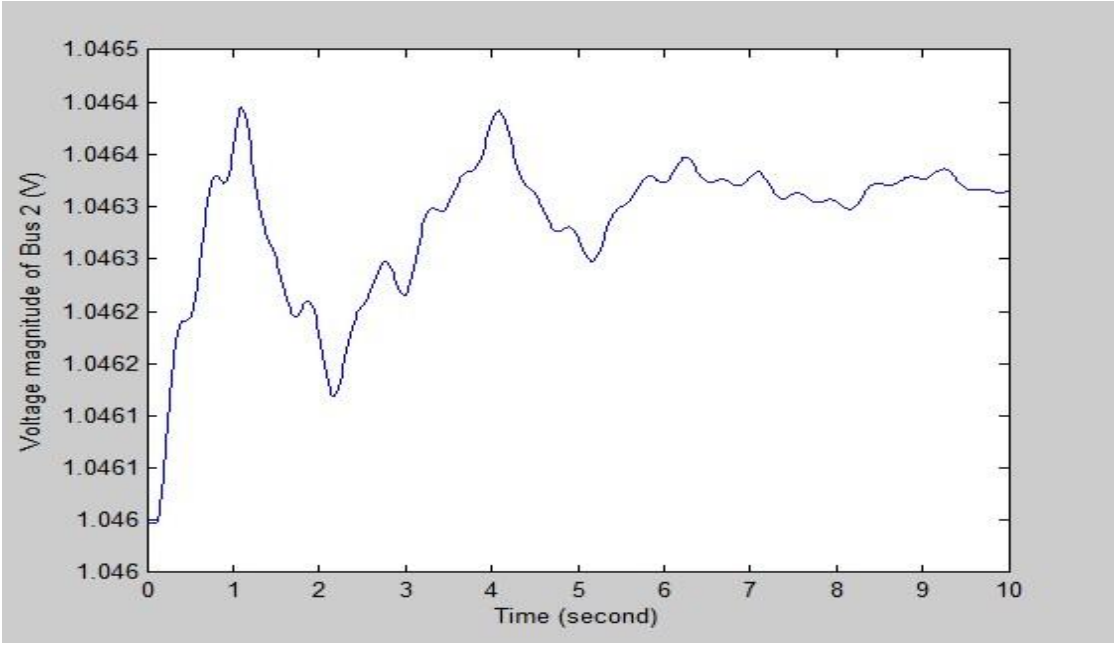

Figure 5.8 Voltage Magnitude of Bus 2

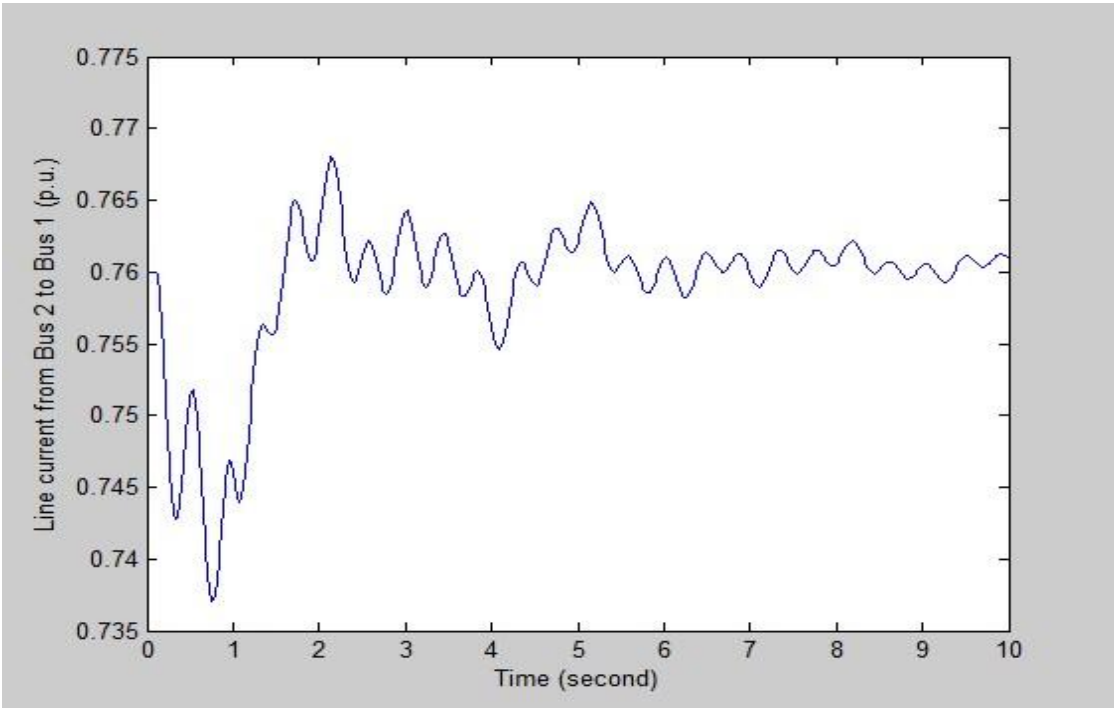

Figure 5.9 Line current Magnitude of Bus 2

B. Power Flow in 68-Bus Power System

Power flow could be calculated based on the PMUs' output of line current and voltage current with their phasors. The power flow including the real power and reactive power could be calculated using the equation expressed below [31, 32]:

$$P = V \bullet I \bullet \cos(\theta - \phi) \tag{5.6}$$

$$Q = V \bullet I \bullet \sin(\theta - \phi) \tag{5.7}$$

Where θ, ϕ refer to the phasor of voltage and line current. Since line current and bus voltage are already obtained from PMUs, the apparent power sending from Bus 2 to Bus 1 is shown in Figure 5.10. The real power and reactive power sending from Bus 2 to Bus 1 are presented in Figure 5.11 and 5.12 respectively.

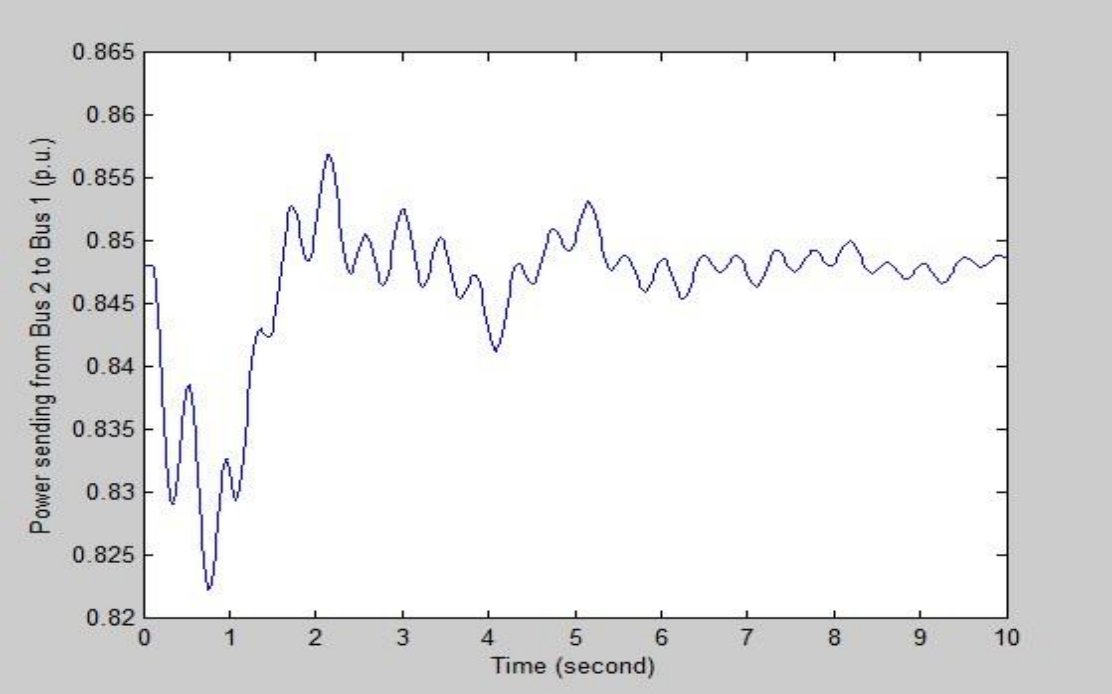

Figure 5.10 Apparent Power through Bus 2 and Bus 1

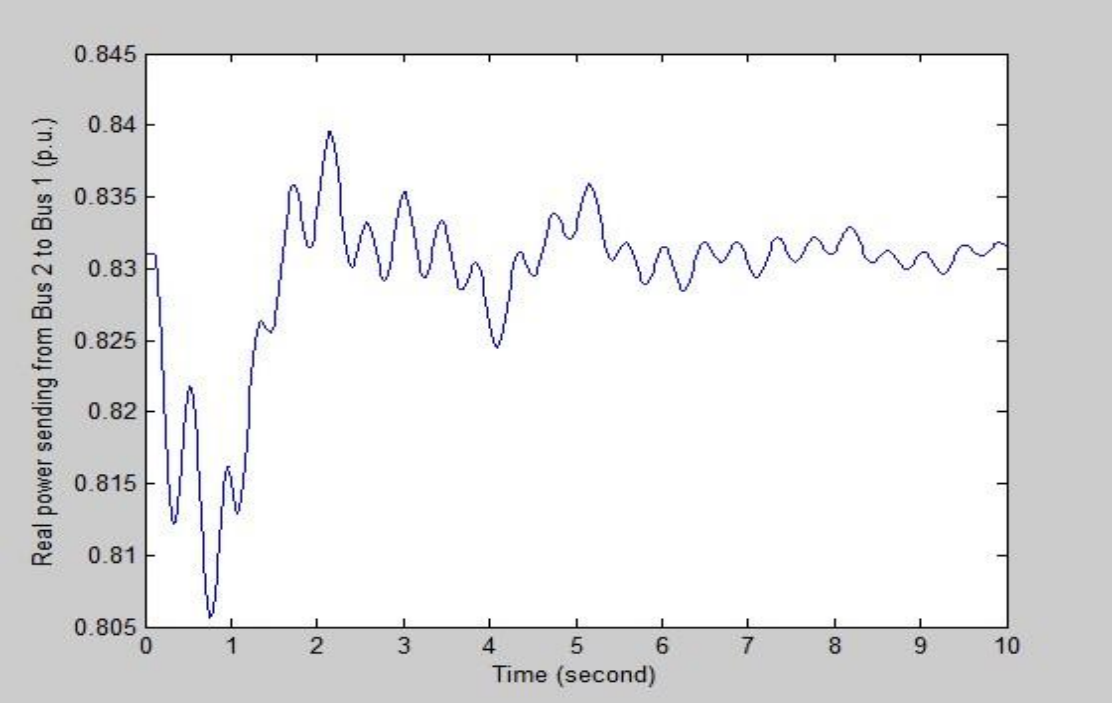

Figure 5.11 Real Power through Bus 2 and Bus 1

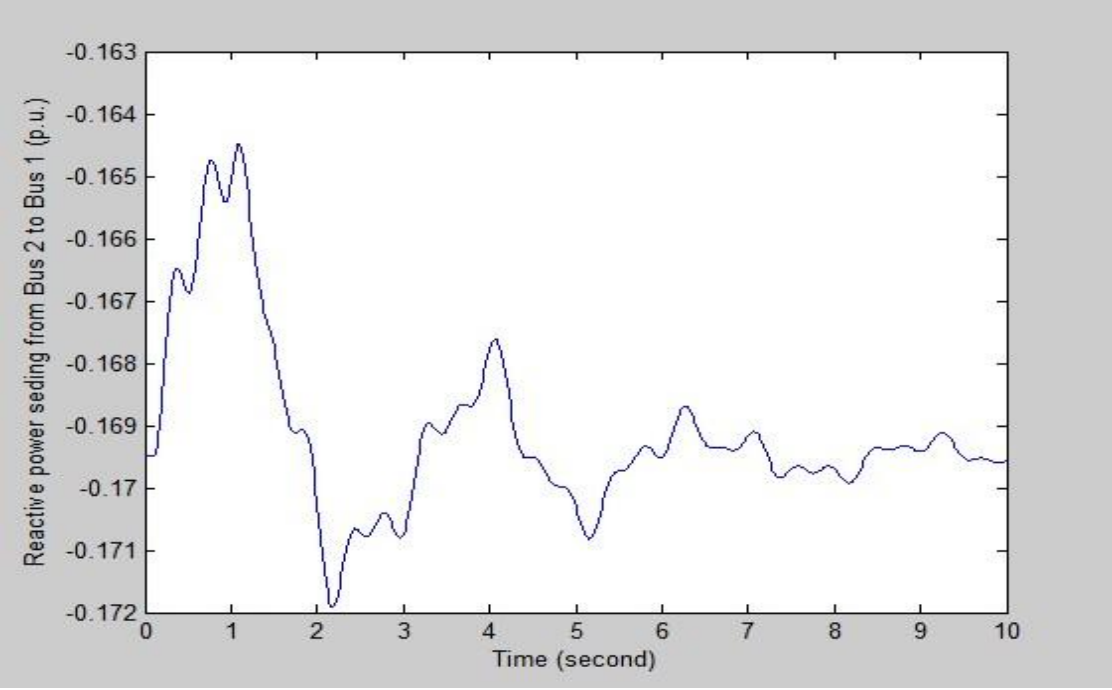

Figure 5.12 Reactive Power through Bus 2 and Bus 1

C. Oscillation Mode of Phasor for Bus Voltages in 68-Bus Power System

Based on wide-area measurements from PMUs installed at various buses, prony method gives the mode of power oscillations. In Figure 5.13, the phasors for bus voltages at Bus 1, 2, 47, 48 are analyzed using prony method, damping of the phasor of each bus is shown. The damping initially is negative, but as the oscillation becomes less, the damping becomes positive and increasing. The positive value of damping is not large, the affect shown in Figure 5.13 is not so obvious. However, the oscillations is decreasing because of the increasing damping. Prony analysis could estimate the damping based on the high accuracy. Synchrophasor measurements are collected from every location in the whole grid with the time stamp based on the speedy communication link, prony method could offer real-time analysis for the data collected from phasor data concentrator. Thus, the mode of every variable is estimated and shown in order to see if there is unstable situation, such as small signal disturbance.

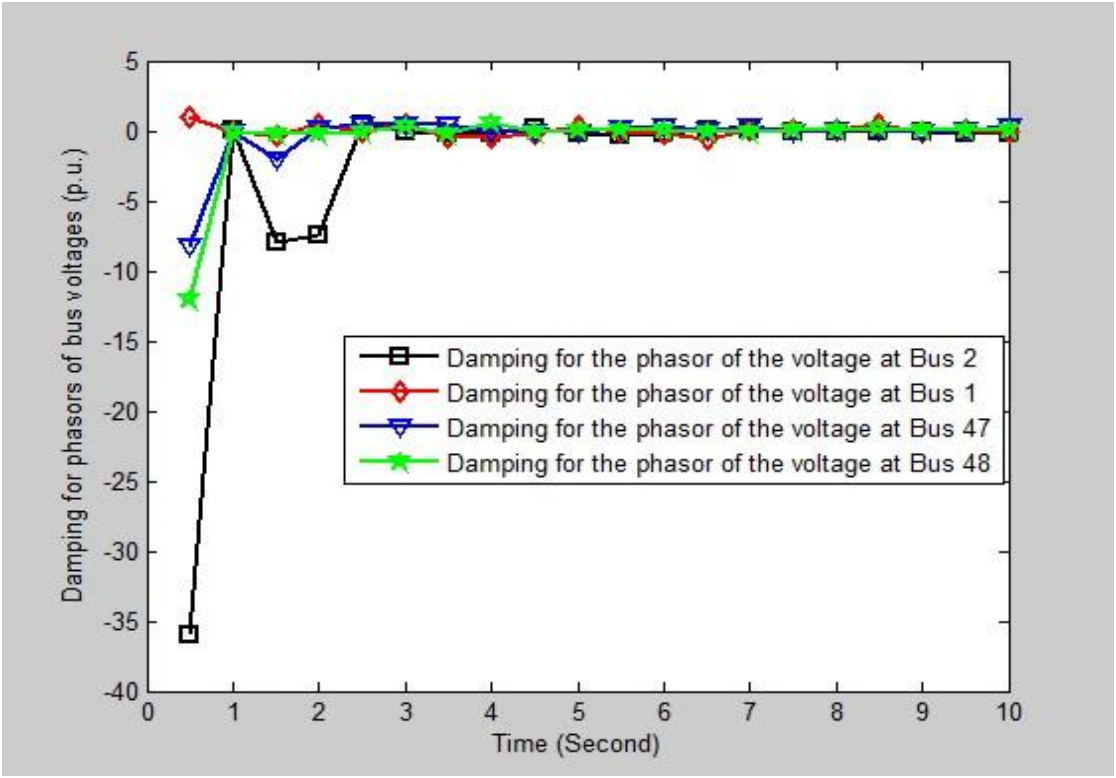

Figure 5.13 Damping for Phasors of Bus Voltages in 68-Bus Power System

5.3.2 Measurement-Based Analysis for 39-Bus Power System

In this section, the 39-bus power system is simulated with inter-area oscillation happened in area 1 and area 2. The mechanical torques of generator 1 and 9 are changed. The torque for generator 1 is decreased by 0.01, the torque for generator 9 is increased by 0.01.

A. Bus Voltage in Two Areas With Inter-Area Oscillation

Inter-area oscillations are the oscillations happened in low frequency within the range of 0.1 to 0.8 Hz. The interconnected power system suffers inter-area oscillations because of the weak tie lines in the large power system. Therefore, the low frequency oscillations take place at groups of generators on one side of the tie line and the other

groups of generators on the other side of the tie line. As the models used for calculating the modes are very complex because of large number of generators, the measurement-based analysis for inter-area oscillation for power system is very effective to detect the modes [37].

In order to observe the inter-area oscillation and analyze the modes for power system's inter-area oscillation, the mechanical toque for generator 1 is increased by 0.01 and decreased by 0.01 for generator 9. The bus voltages at bus 3 and 4 are shown in Figure 5.14 and Figure 5.15. Bus 3 and bus 4 are in area 1 and area 2 respectively, they are connected through a tie line between the two areas. The disturbances are occurred in these two areas. The oscillations for the bus voltages shown in the two figures are in the decreasing trend and with low frequency. The system is not stable because of the inter-area oscillations.

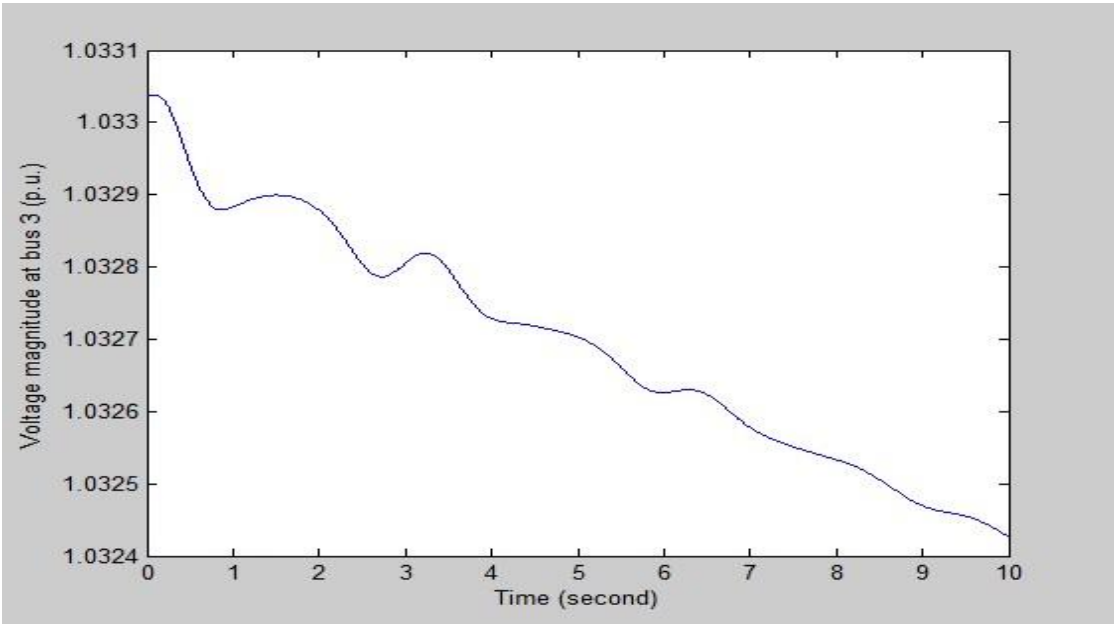

Figure 5.14 Voltage Magnitude at Bus 3

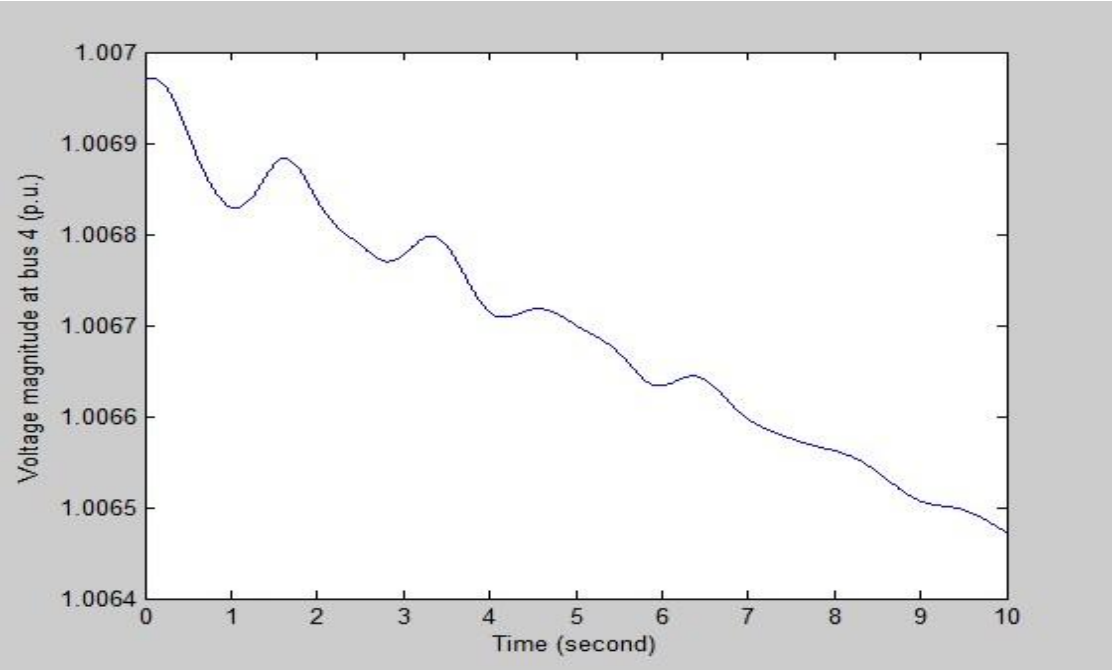

Figure 5.15 Bus Magnitude at Bus 4

B. Frequency and Damping Estimation for the Oscillated Bus Voltages

The frequency and damping estimation for measurement-based analysis is based on prony estimation method. The estimation is captured with the real-time measurement from PMU installed nearby. The frequency for the oscillations is shown in Figure 5.16. Because the system has inter-area oscillation, the frequency should below 0.8 Hz. The estimated value in Figure 5.16 verifies the nature of the oscillation. Most of the estimated values are below 0.8 Hz.

The damping for the oscillations at two buses are shown in Figure 5.17. Since the oscillation is in a decreasing trend, the estimated damping values are in an increasing trend. Initially, the oscillation is poorly damped, so the estimated damping value is very negative, however, the oscillation is not intense as the time variation, the

estimated damping value is close to positive part, which indicates the decreasing oscillation trend [38].

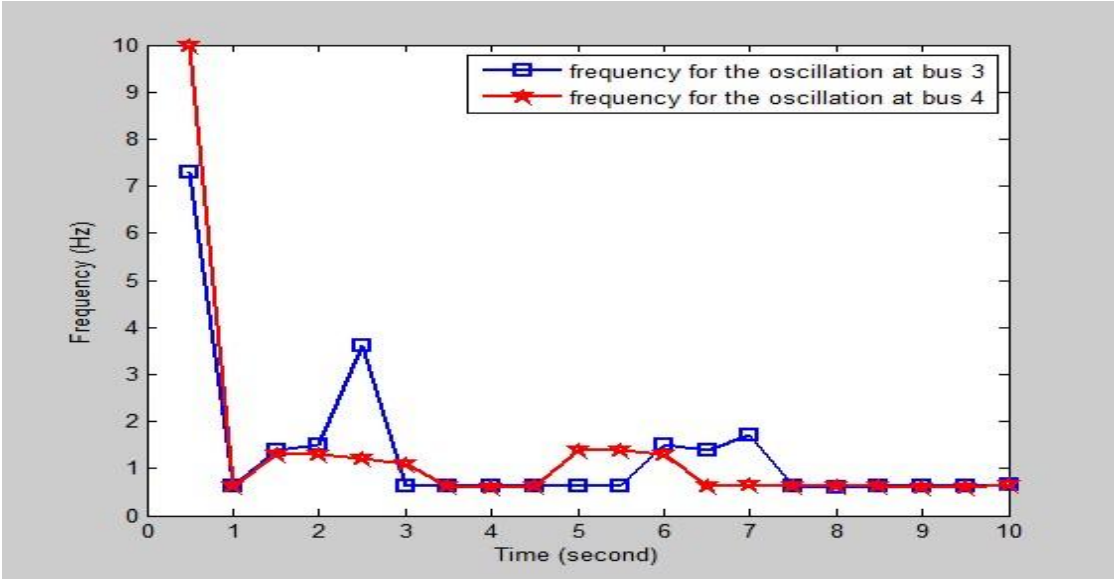

Figure 5.16 Frequency for the Oscillations at Bus 3, 4

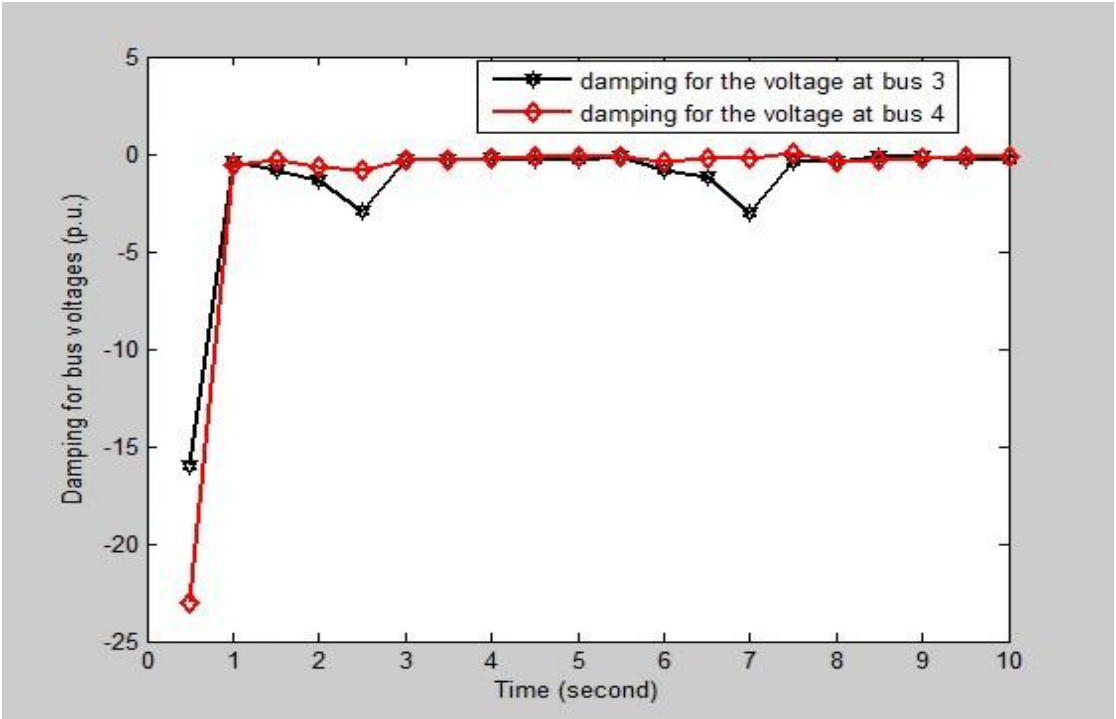

Figure 5.17 Damping for Bus Voltages at Bus 3, 4

5.4 Measurement-Based Analysis Technique's Deployment in Power System

Measurement-based analysis technique has been used for Oscillation Monitoring System (OMS) to detect the oscillation happened both in local mode and inter-area mode situations. The system is developed by Washington State University. OMS controller could control the trigger and detect the mode damping levels and shape. When the system happens the small and medium disturbance, the damping and frequency are estimated using three algorithms in OMS controller, if the value of damping and frequency is lower than the threshold, the command for the alert and trigger is activated based on the type of disturbance. According to the specific type of oscillation, the central unit will determine the type of method that could be used for stabilizing the system [39]. This section only introduces the general measurement-based technique that is applied in power system.

For OMS, three algorithms are applied to process the measurement data captured from PMUs, they are prony method, Matrix Pencil method and Hankel Total Least Square (HTLS) method. In this thesis, only prony method is used for illustrating the measurement-based analysis technique. These three algorithms are used to detect the frequency, damping and mode shape of oscillation. These three methods can all be used for detecting the phasor, the results are more accurate than using only one method. Matrix pencil and HTLS are explained with details in [15]. As power oscillation happened during the disturbance includes the linear and nonlinear data, it is not easy for prony method to detect the accurate information for the modes. OMS

contains the crosscheck rules to ensure the data estimated in the system is accurate and reliable to issue the command. The crosscheck rules are applied to the real-time windows, different signal groups and different algorithms [40].

OMS supports local area oscillation estimation and inter-area oscillation estimation. For local area oscillation, the measurement used for the three methods is obtained from the same PMU. For inter-area oscillation, the measurement is obtained from the PMUs that have participated the oscillation during disturbance. In order to apply crosscheck rules after the estimation in the three engines, the crosscheck rules are used in local area oscillation and inter-area oscillation respectively. For local area oscillation, the estimation result is regarded as consistent if the three methods' results are all showed in the same range. For inter-area oscillation, Inter-area mode and inter-area moving window crosscheck are used for crosscheck. Inter-area mode crosscheck shows the oscillation from different PMUs with the same frequency. Inter-area moving window crosscheck compares the data from several moving windows. The simplified flowchart is shown in Figure 5.18 [40].

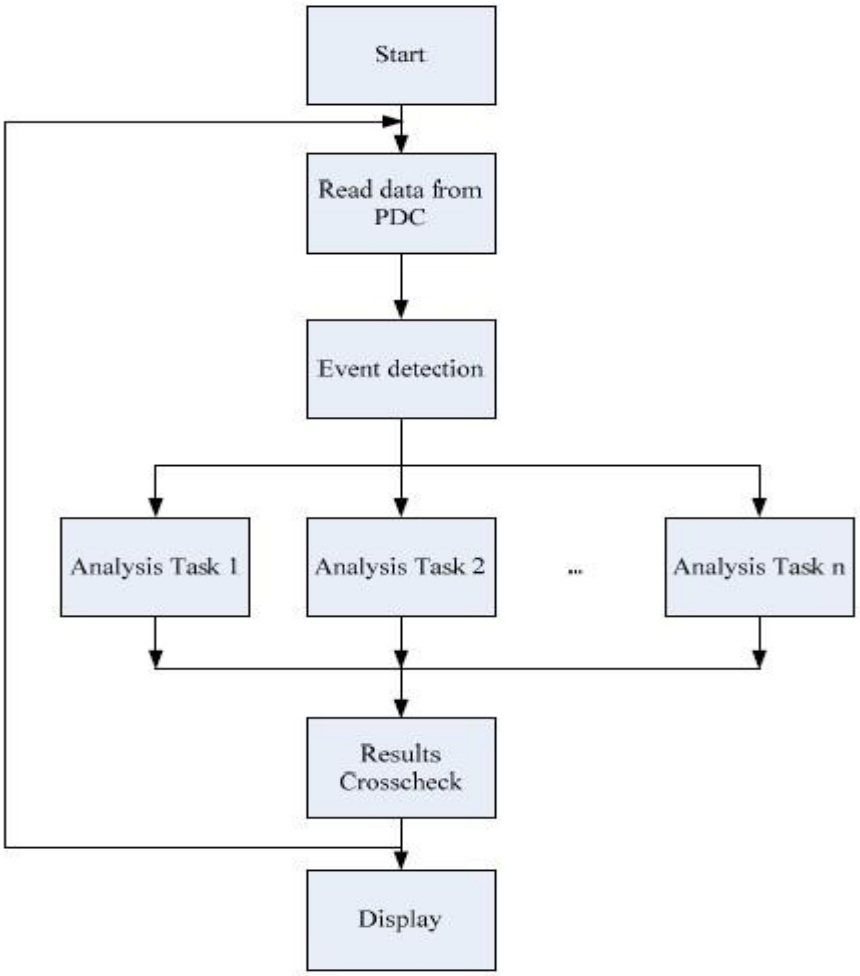

Figure 5.18 Simplified Flowchart for OMS [40]

5.5 Conclusion

The chapter discusses the measurement-based analysis and its application for large power system. Using DFT method to calculate phasors for line current and bus voltage could accurate measure the system and make the whole system visible. The measurements get from every location at the same time supports the oscillations' mode analysis. The damping and frequency of oscillation can be shown to detect if there is a sudden oscillation in the system.

Chapter 6

Conclusion and Future Works

6.1 Conclusions

Small disturbance causes the small signal stability problem, which result in local-area oscillation and wide-area oscillation. The determination of power system stability is important during the operation. Model-based analysis for small signal stability problem uses eigenvalue analysis to detect the power system stability. However, the method is not in real-time and suitable for the highly dynamic power system. The need of real-time analysis from every location and the visualization of power system is important. The thesis provides the theory of both conventional method (model-based analysis) and advanced method (measurement-based analysis), and shows the effectiveness of measurement-based analysis.

Measurement-based can provide real-time analysis through synchrophasor measurement collected from PMUs. The measurements are noted with time stamp from every location in the system which make the whole system visualized. Based on the real-time measurements obtained from DFT method, the damping of the oscillation could be estimated by prony method.

Measurement-based analysis is closer to the dynamic environment for power system compared to the conventional method. The performances of two different methods are compared through various case studies. By using measurement-based method for analyzing small signal stability problem in power system, the amplified trend of oscillation will be detected before it becomes worse.

6.2 Contribution of the Thesis

1. The study of the phenomenon caused by small disturbance and the reasons that lead to small signal stability problem.
2. The investigation of model-based method for analyzing small signal stability problem and the mathematical model used in the method.
3. The study on measurement-based method for analyzing small signal stability problem.
4. The complete analysis for prony estimation used in measurement-based method.
5. Research on PMUs' principle, function and application used in power system.
6. Applications for measurement-based method to various systems with the study in Power System Toolbox, Power System Analysis Toolbox, Prony Toolbox.

6.3 Future Works

This thesis mainly focus on the methods of analyzing the oscillation caused by small signal stability problem. The different effects of applying two methods are illustrated in the thesis. The future research will focus on the synchrophasor

measurement.

Synchrophasor measurements make the whole system become visualized, and it is the media for realizing the measurement-based analysis. The main challenge for synchrophasor measurements is find the optimum algorithm to select locations for PMUs to collect the data. The purpose is to use the minimum numbers of PMUs to make the whole power system visualized. The optimum placement of PUMs is part of the future work.

Since power system is highly interconnected and widely distributed, the number of blackouts will be reduced if the protective system uses synchrophasor measurements. The power system's reliability for power generation, transmission, distribution and networks will be increased. The protection for power system will be more intelligent. Future research on implementing suitable controls based on small signal stability analysis will be useful [33].

References

[1] P. Kundur and L. Wang, "Small signal stability analysis: experiences, achievements, and challenges," *Power System Technology. 2002. Proceedings. Power Con 2002. International Conference*, Kunming, China, Vol. 1, pp. 6-12. October 2002.

[2] P. Kundur, J. Paserba, V. Ajjarapu, G.Andersson, A. Bose, C. Canizares, N. Hatziargyriou, D. Hill, A. Stankovic, C. Taylor, T. V. Cutsem, and V. Vittal, "Definition and classification of power system stability," *IEEE Trans. Power Systems*, vol. 19, no. 2, pp. 1387-1401, May 2004.

[3] P. Kundur, *Power System Stability and Control*, New York: McGraw Hill, 1994.

[4] Pai, M. A., and D. P. Gupta. *Small signal analysis of power systems*. Harrow, Middlesex: Alpha Science International, 2004.

[5] G. Rogers, *Power System Oscillations*, Boston: Kluwer Academic, 2000.

[6] Westinghouse Electric Corporation, *Electrical transmission and distribution reference*, Westinghouse Electric & Manufacturing Company, 1942.

[7] IEEE Recommended Practice for Excitation System Models for Power System Stability Studies, IEEE Std 421.5™-2005, 21 April 2006.

[8] F. P. Demello and C. Concordia, "Concepts of Synchronous Machine Stability as Affected by Excitation Control," *IEEE Trans. Power Apparatus and Systems*, Vol. PAS-88 . pp.316-329, No.4, April 1969.

[9] F. Milano, *Power System Modelling and Scripting*, London, Toronto: Springer, 2010.

[10] C.M Ong, *Dynamic Simulation of Electric Machinery*, Upper Saddle River, New Jersey: Prentice Hall, Inc. 1998.

[11] F. Milano, PSAT, Free Software Foundation, July 14, 2005

[12] Power System Analysis Toolbox, version 2.1.6, F. Milano, May 13,1010

[13] A. Ragavendiran and R. Gnanadass, "Determination of Location and Performance Analysis of Power System Stabilizer Based On participation Factor," Electrical, Electronics and Computer Science (SCEECS), IEEE Students' Conference, Bhopal, pp. 1-9, March 2012.

[14] Z. Y. Dong. "Stability Analysis and Control in Modern Power Systems" Ph.D. Dissertation, Faculty of Engineering, University of Sydney, Australia, 1998.

[15] G. Liu, "Oscillation monitoring system based on wide area phasor measurements in power systems," Ph.D. Dissertation, Dept. Electrical Engineering and Computer Science, Washington State Univ., USA, 2010.

[16] Power System Toolbox, version 2.0, Cheery Tree Scientific Software, Canada, 1991.

[17] A. G. Phadke and J. S. Thorp, *Synchronized Phasor Measurements and Their applications*, New York: Springer, 2008.

[18] A. G. Phadke and R.M. de Moraes, "The wide world of wide-area measurement," *IEEE Power & Energy Magazine*, vol. 6, No. 5, pp. 52-65, September/October 2008.

[19] S. Chakrabarti, E. Kyriakides, B. Tianshu, D. Cai, V. Terzija, "Measurements get together," *IEEE Power & Energy Magazine*, vol. 7, No. 1, pp. 41-49, January/February 2009.

[20] J. D. L. Ree, V. Centeno, J. S. Thorp, and A. G. Phadke, "Synchronized phasor measurement applications in power systems," *IEEE Trans. Smart Grid*, vol. 1, No. 1, pp. 20 - 27, June 2010.

[21] K, Martin, and J, Carroll, "Phasing in the technology," *IEEE Power & Energy Magazine*, vol. 6, No. 5, pp. 24-33, September/October 2008.

[22] J. Thorp, A, Abur, M. Begovic, J. Giri, R. Avila-Rosales, " Gaining a wider perspective," *IEEE Power & Energy Magzine*, vol. 6, No. 5, pp. 43-51, September/October 2008.

[23] Working Group H-7 of the Relaying Channels and Subcommittee of the IEEE Power System Relaying Committee, "Synchronized sampling and phasor measurements for relaying and control," *IEEE Trans. Power Delivery*, Vol. 9, No. 1, pp. 442 - 452, January 1994.

[24] A. Gomez-Exposito, A. Abur, P. Rousseaux, A. de la Villa Jaen, and C. Gomez-Quiles, "On the use of PMUs in power system state estimation," in *Proc. 17th Power Systems Computation Conference,* Stockholm, Sweden, August 2011.

[25] M.Sherwood, D. Hu and V.Venkatasubramanian, "Real-time detection of angle instability using synchrophasors and action principle", Bulk Power System Dynamics and Control-VII, Charleston SC., pp. 1-11, August 2007.

[26] V. M. Venkatasubramanian, X. Liu, G. Liu, Q. Zhang, and M. Sherwood," Overview of wide-area stability monitoring algorithms in power systems using synchrophasors," in *Proc. American Control Conference (ACC),* San Francisco, CA, pp. 4172-4176, June 2011.

[27] M. Patel, et al., *Real-Time Application of Synchrophasors for Improving Reliability,* Princeton, New Jersey: North Amerian Electric Reliability Corperation, 2010.

[28] E. O. Schweitzer, D. Whitehead, A. Guzman, Y. Gong and M. Donolo. (2008). Schweitzer Engineering Laboratories. Pullman, USA. [Online]. Available: https://www.selinc.com/literature/TechnicalPapers/.

[29] E. D. Tuglie, M. Dicorato, F. Torelli and M. Trovato, "Improving maximum loadability of multiple transaction-based markets by system losses reconfiguration," in *Proc. Transmission & Distribution Conference and Exposition: Latin America* , Caracas, pp. 1-6, August 2006.

[30] T. L. Baldwin L. Mili M. B. Boisen, and Jr. R. Adapa, "Power system observability with minimal phasor measurement placement," *IEEE Trans. Power Systems,* Vol. 8, No. 2, pp. 707-715, May 1993.

[31] K. Martin, "Synchrophasor solutions for the smart grid," presented at the 2011 Conf. Electrical Power and Energy, Winnipeg, CA, Oct. 3-5, 2011.

[32] J. D. Glover, M. S. Sarma, and T. J. Overbye, *Power System Analysis and Design Fifth Edition,* Stamford, USA: Cengage Learning, 2011.

[33] V. Terzija, et al., "Wide-area monitoring, protection, and control of future electric power networks," *Proceedings of the IEEE,* vol. 99, pp. 80-93, January 2011.

[34] A. P. S. Meliopoulos and G. J. Cokkinides, "Advanced synchrophasor application," *In Proc. Power and Energy Society General Meeting,* Minneapolis,

MN, July 2010, pp. 1-6.

[35] E. Vittal, M. O'Malley and A. Keane, "A small-signal stability analysis of DFIG wind generation." in *Proc. 8th International Workshop on Large-Scale Integration of Wind Power into Power Systems*, 2009.

[36] A-R. A. Khatib, "Internet-based wide area measurement applications in deregulated power systems," Ph.D. dissertation, Dept. Electrical and Computer Engineering, Virginia Polytechnic and State University, Virginia , 2002.

[37] M. Klein, G.J. Rogers and P. Kundur, "A fundamental study of inter-area oscillations in power systems," *IEEE Trans. Power Systems*, *v*ol. 6, pp. 914-921, Aug. 1991.

[38] K. Uhlen, L. Warland, J. O. Gjerde, Ø. Breidablik, M. Uusitalo, A. B. Leirbukt and P. Korba, "Monitoring amplitude, frequency and damping of power system oscillations with PMU measurements," in *Proc. Power and Energy Society General Meeting - Conversion and Delivery of Electrical Energy in the 21st Century,* Pittsburgh, PA, pp. 1-7, July 2008.

[39] J. Quintero, G. Liu and V. Venkatasubramanian, "An oscillation monitoring system for real-time detection of small-signal instability in large electric power systems," in *Proc. Power Engineering Society General Meeting*, Tampa, FL, pp. 1-8, June 2007.

[40] G. Liu, J. Quintero and V. Venkatasubramanian, "Oscillation monitoring system based on wide area synchrophasors in power systems," in *Proc. 2007 iREP Symposium,* Charleston, SC, pp. 1-13, August 2007.

[41] B. Pal and B. Chaudhuri, *Robust Control in Power Systems*, U.S: Springer, 2005

Appendix A: Data for Two-Area Power System

Appendix A provides the information for the two-area power system [5] that has been illustrated in the thesis. The system's base is 100 MVA, 230 kV. Figure A.1 gives the single line diagram of the two-area power system, Table A.1 shows the power flow results for the two-area power system [1, 12].

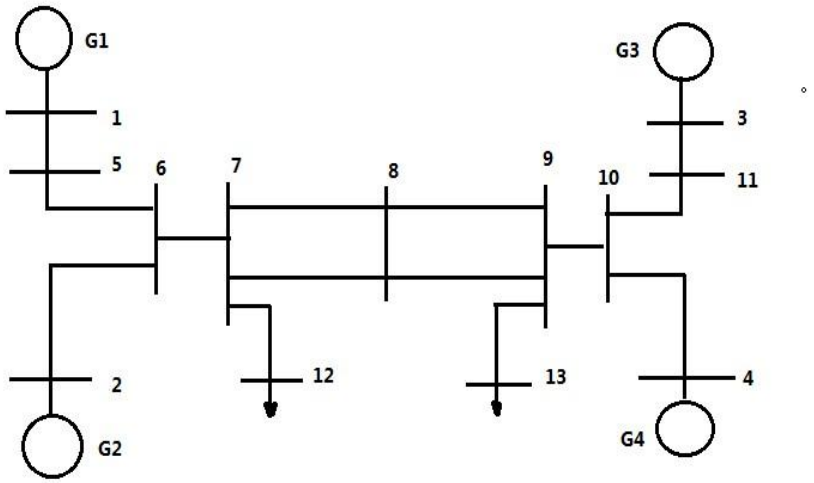

Figure A.1 Single Line Diagram of the Two-Area Power System

Table A.1 Power Flow Results for Two-Area System

Bus	V p.u.	Phase rad	P_G MW	Q_G MVar	Pload MW	Qload MVar
1	1.03	0.35	700	182.45	0	0
2	1.01	0.18	700	0.0665	0	0
3	1.03	-0.12	718.9	-0.109	0	0
4	1.01	-0.29	700	0	0	0
5	1.0	0.24	0	0	0	0
6	0.98	0.06	0	0	0	0
7	0.96	-0.08	0	0	967	100
8	0.95	-0.32	0	0	0	0
9	0.97	-0.56	0	0	1767	250
10	0.98	-0.41	0	0	0	0
11	1.01	-0.23	0	0	0	0
12	0.96	-0.08	0	0	967	100
13	0.97	-0.56	0	0	1767	250

Appendix B: Data for the 4 × 555 MVA Power System

Appendix B contains the data for the 4 × 555 MVA power system which is discussed in the thesis [3]. The system base is 2220 MVA and 24 KV. The real power and reactive power at bus E_t are 0.9 and 0.3 p.u. Figure B.1 gives the single line diagram of this power system and Table B.1 provides the constants for the mathematical model that are used for mode-based analysis for this power system.

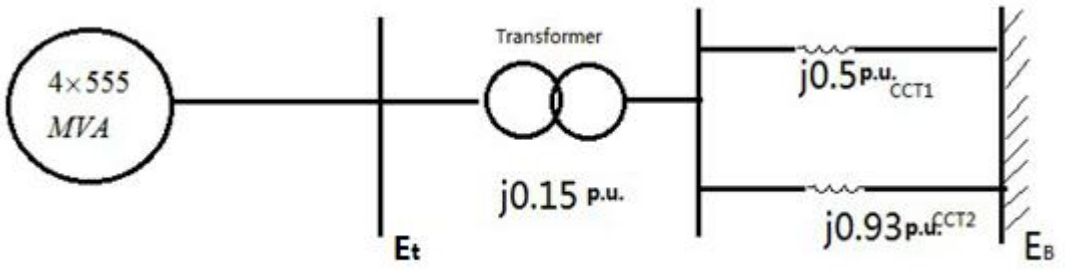

Figure B.1 Single Line Diagram of 4×555 MVA System

Table B.1 Constants for the 4×555 MVA System

K_1	K_2	K_3	K_4	K_5
0.7643	0.8649	0.3230	1.4187	-0.1463
K_6	T_3	T_R	G_{ex}	
0.4168	2.365	0.02	200	

Appendix C: Data for the IEEE 14-Bus Power System

Appendix C gives the information for the IEEE 14-bus power system that presented in Chapter 3 in this thesis [12, 9]. Figure C.1 contains the single line diagram of the IEEE 14-bus power system, Table C.1 gives the load information for this power system, the synchronous generators' and automatic voltage regulators' information are shown in Table C.2 and Table C.3 respectively. The system's power base is 100 MVA, for the purpose of calculation convenience, regarding to the bus 1 to 5, the voltage basis is 69 kV, for the bus 6, 7 and 9 to 14, voltage base is 13.8 kV, for the bus 8, voltage base is 18 kV.

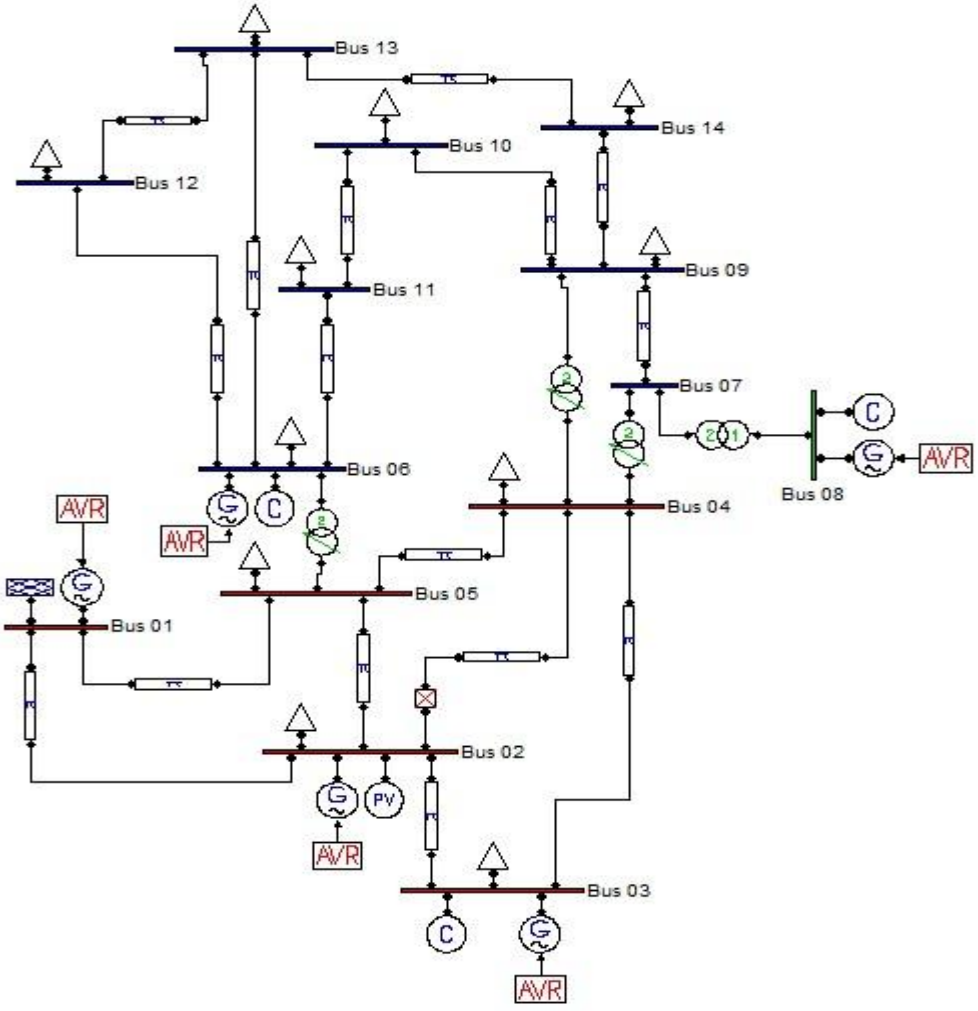

Figure C.1 Single Line Diagram of IEEE 14-Bus Power System [12]

Table C.1 Constant PQ Load Information For IEEE 14-Bus System

Bus Number	Voltage Base (kV)	Real Power (MW)	Reactive Power (MVAR)
1	69	-	-
2	69	12.7	12.7
3	69	94.2	19
4	69	47.8	-3.9
5	69	7.6	1.6
6	13.8	11.2	7.5
7	13.8	-	-
8	18	-	-
9	13.8	29.5	16.6
10	13.8	9	5.8
11	13.8	3.5	1.8
12	13.8	6.1	1.6
13	13.8	13.5	5.8
14	13.8	14.9	5

Appendix D: Data for the 68-Bus Power System

Appendix D contains the information for the 68-Bus Power System that is discussed in Chapter 5 in this thesis [5]. Table D.1 gives the load information at various buses in this system. The system base is 100 MVA .

Table D.1 Load Information for the 68-Bus Power System

Bus No.	1	3	4	7	8	9
P(MW)	252.7	322	500	234	522	104
Q(MVAR)	118.56	2	184	084	177	125
Bus No.	12	15	16	18	20	21
P(MW)	9	320	329	158	680	274
Q(MVAR)	88	153	32	30	103	115
Bus No.	23	24	25	26	27	28
P(MW)	248	309	224	139	281	206
Q(MVAR)	85	-92	47	17	76	28
Bus No.	29	33	36	37	39	40
P(MW)	284	112	102	6000	267	65.63
Q(MVAR)	27	0	-19.46	300	12.6	23.53
Bus No.	41	42	44	45	46	47
P(MW)	1000	1150	267.55	208	150.7	203.12

Q(MVAR)	250	250	4.84	21	28.5	32.59
Bus No.	48	49	50	51	52	
P(MW)	241.20	164.0	100	337	2470	
Q(MVAR)	2.2	29	-147	-122	123	

Table D.2 Synchronous Machine Information for 68-Bus Power System

No.	Bus Connected	x_d' (p.u.)	T_{q0}' (sec.)
SynM 1	53	0.031	42
SynM 2	54	0.0697	30.2
SynM 3	55	0.0531	35.8
SynM 4	56	0.0436	28.6
SynM 5	57	0.066	26
SynM 6	58	0.05	34.8
SynM 7	59	0.0049	26.4
SynM 8	60	0.057	26.3
SynM 9	61	0.057	34.5
SynM 10	62	0.0457	31.0
SynM 11	63	0.018	28.2
SynM 12	64	0.037	92.3
SynM 13	65	0.0055	248.0
SynM 14	66	0.00285	300.0
SynM 15	67	0.00285	300.0
SynM 16	68	0.0071	225.0

Appendix E: Data for the 39-Bus Power System

Appendix E gives the data for the 39-bus power system that is used in Chapter 5 [36]. Table E.1 provides the bus data for this system. Table E.2 gives the load data for the 39-bus power system. Table E.3 includes the generators' information for this power system. The system is based on 100 MVA, 60 Hz and 100 kV.

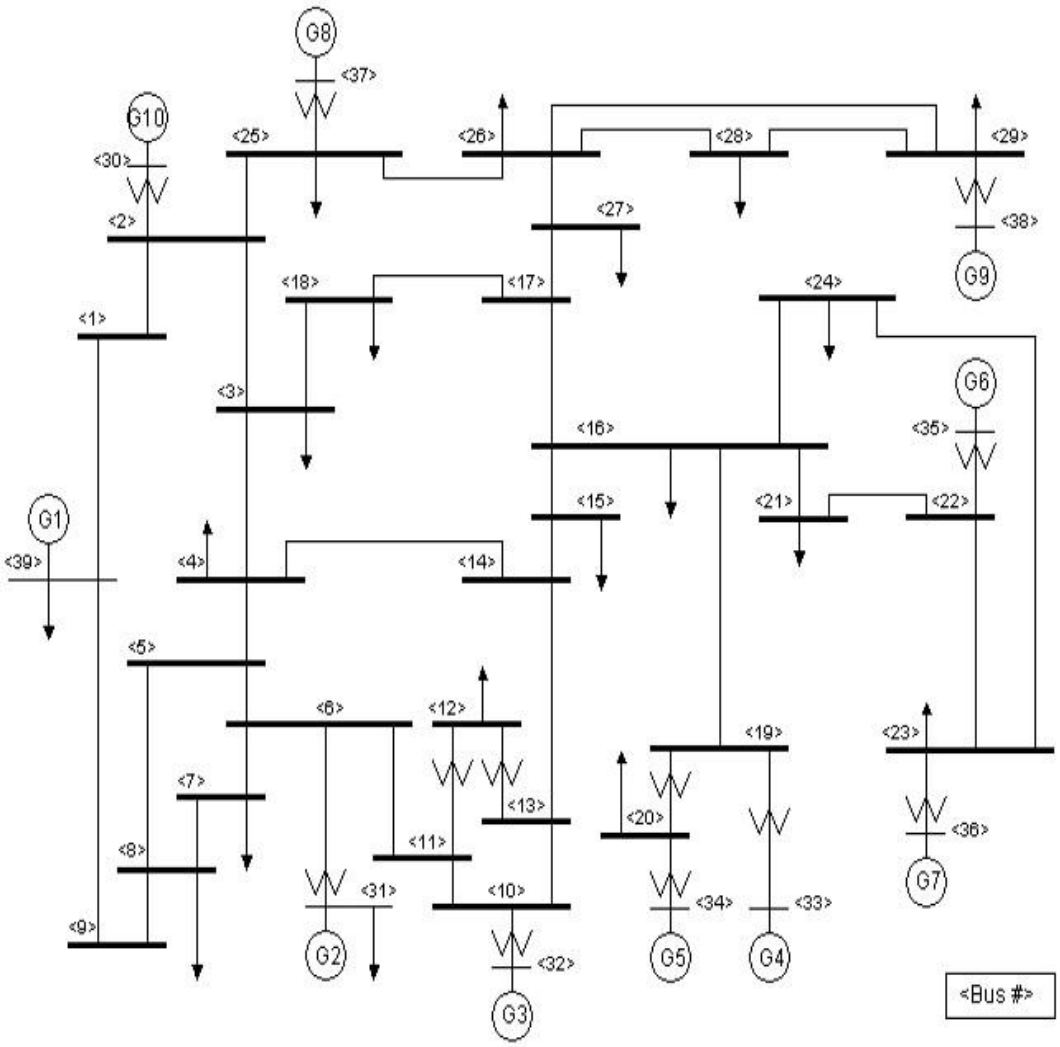

Figure E.1 Single Line Diagram of 39-Bus Power System [36]

Table E.1 Bus Data for 39-Bus Power System [36]

Bus No.	GL	BL	Bus Voltage Magnitude (p.u.)	Bus angle (degree)
1	0	0	1.04754	-9.5707
2	0	0	1.04896	-7.0111
3	0	0	1.03042	-9.8581
4	0	0	1.00381	-10.6546
5	0	0	1.00502	-9.4687
6	0	0	1.00736	-8.7668
7	0	0	0.9967	-10.9762
8	0	0	0.99573	-11.4762
9	0	0	1.02809	-11.2997
10	0	0	1.01702	-6.3816
11	0	0	1.01253	-7.1952
12	0	0	1	-7.2106
13	0	0	1.01419	-7.0959
14	0	0	1.01173	-8.7648
15	0	0	1.01578	-9.1807
16	0	0	1.03225	-7.7766
17	0	0	1.03395	-8.7748
18	0	0	1.03129	-9.6156
19	0	0	1.05001	-3.1525
20	0	0	0.99096	-4.5639
21	0	0	1.0321	-5.371
22	0	0	1.04998	-0.9239

23	0	0	1.04998	-1.1221
24	0	0	1.03775	-7.657
25	0	0	1.05752	-5.6492
26	0	0	1.05215	-6.9058
27	0	0	1.03795	-8.9173
28	0	0	1.05016	-3.3942
29	0	0	1.04997	-0.6351
30	0	0	1.0475	-4.9818
31	0	0	0.982	0
32	0	0	0.9831	1.6155
33	0	0	0.9972	2.0647
34	0	0	1.0123	0.6263
35	0	0	1.0493	4.037
36	0	0	1.0635	6.7296
37	0	0	1.0278	1.1355
38	0	0	1.0265	6.4282
39	0	0	1.03	-11.1082

Table E.2 Load Data for 39-Bus Power System

Bus No.	Pload (MW)	Qload (MVar)
3	322	2.4
4	500	184
7	233.8	84
8	522	176
12	8.5	88
15	320	153
16	329	32.3
18	158	30
20	680	103
21	274	115
23	247.5	84.6
24	308.6	-92.2
25	224	47.2
26	139	17
27	281	75.5
28	206	27.6
29	283.5	26.9
31	9.6	4.6
39	1104	250

Table E.3 Generator Data for 39-Bus Power System

Generator No.	H	r_a *p.u.*	x_d' *p.u.*	x_q' *p.u.*	x_d *p.u.*	x_q *p.u.*	T_{d0}' *sec*	T_{q0}' *sec*	xl *p.u.*
1	500	0	0.006	0.008	0.02	0.019	7	0.7	0.003
2	30.3	0	0.0697	0.17	0.0295	0.282	6.56	1.5	0.035
3	35.8	0	0.0531	0.0876	0.2495	0.237	5.7	1.5	0.030
4	28.6	0	0.0436	0.166	0.262	0.258	5.69	1.5	0.029
5	26	0	0.132	0.166	0.67	0.62	5.4	0.44	0.054
6	34.8	0	0.05	0.0814	0.254	0.241	7.3	0.4	0.022
7	26.4	0	0.049	0.186	0.295	0.292	5.66	1.5	0.032
8	24.3	0	0.057	0.0911	0.290	0.28	4.7	0.41	0.028
9	34.5	0	0.057	0.0587	0.2106	0.205	4.79	1.69	0.029
10	42	0	0.031	0.008	0.1	0.069	10.2	0	0.012

Conference Papers during the MEng Program

During my MEng program, I have completed four conference papers listed as below:

1. D. Lin and B. Jeyasurya, "Application of Model Predictive Control in Power System," Newfoundland Electrical and Computer Engineering Conference, St.John's, Newfoundland, November 2012.

2. D. Lin and B. Jeyasurya, "Measurement-Based Analysis of Power System Small Signal Stability," Electrical Power & Energy Conference (EPEC), Halifax, Nova Scotia, August 2013.

3. D. Lin, R. Hadidi and B. Jeyasurya, "Power System Small-Signal Stability: Analysis and Use of Wide-Area Monitoring Systems," International Council on Large Electric Systems (CIGRE) Canada Conference, Toronto, September 2014.

4. D. Lin and B. Jeyasurya, "Power System Small Signal Stability Analysis: Theoretical Foundations and Recent Advances," Newfoundland Electrical and Computer Engineering Conference, St.John's, Newfoundland, November 2014.